Effects of central metal ion (Mg, Zn) and solvent on singlet excited-state energy flow in porphyrin-based nanostructures

Feirong Li,[a] Steve Gentemann,[b] William A. Kalsbeck,[c] Jyoti Seth,[c] Jonathan S. Lindsey,*[a] Dewey Holten*[b] and David F. Bocian*[c]

[a]*Department of Chemistry, North Carolina State University, Raleigh, NC 27695–8204, USA*
[b]*Department of Chemistry, Washington University, St. Louis, MO 63130–4899, USA*
[c]*Department of Chemistry, University of California, Riverside, CA 92521–0403, USA*

Zinc porphyrins have been widely used as surrogates for chlorophyll (which contains magnesium) in photosynthetic model systems and molecular photonic devices. In order to compare the photodynamic behaviour of Mg- and Zn-porphyrins, dimeric and star-shaped pentameric arrays comprised of free-base (Fb) and Mg- or Zn-porphyrins with intervening diarylethyne linkers have been prepared. A modular building block approach is used to couple ethynyl- or iodo-substituted porphyrins in defined metallation states (Fb, Mg or Zn) *via* a Pd-catalysed reaction in 2–6 h. The resulting arrays are purified in 45–80% overall yields by combinations of size exclusion chromatography and adsorption chromatography ($\geqslant$95% purity). High solubility of the arrays in organic solvents facilitates chemical and spectroscopic characterization. The star-shaped Mg_4Fb- and Zn_4Fb-pentamers, where the Fb-porphyrin is at the core of the array, have pairwise interactions similar to those of dimeric MgFb- and ZnFb-arrays. The arrays have been investigated by static and time-resolved absorption and fluorescence spectroscopy, as well as resonance Raman spectroscopy. The major findings include the following. (1) The rate of singlet excited-state energy transfer from the Mg-porphyrin to the Fb-porphyrin [$(31\ ps)^{-1}$] is comparable to that from the Zn-porphyrin to the Fb-porphyrin [$(26\ ps)^{-1}$] in the dimeric arrays. Qualitatively similar results are obtained for the star-shaped pentamers. The similar rates of energy transfer for the Mg- and Zn-containing arrays are attributed to the fact that the electronic coupling between the metalloporphyrin and Fb-porphyrin is approximately the same for Mg- *vs.* Zn-containing arrays. (2) The quantum yield of energy transfer is slightly higher in the Mg-arrays (99.7%) than in the Zn-arrays (99.0%) due to the longer inherent lifetime of Mg-porphyrins (10 ns) compared with Zn-porphyrins (2.5 ns). (3) The rate of energy transfer and the magnitude of the electronic coupling are essentially independent of the solvent polarity and the coordination geometry of the metalloporphyrin (four- or five-coordinate for Zn-porphyrins, five- or six-coordinate for Mg-porphyrins). (4) Polar solvents diminish the fluorescence yield and lifetime of the excited Fb-porphyrin in arrays containing either Mg- or Zn-porphyrins. These effects are attributed to charge-transfer quenching of the Fb-porphyrin by the adjacent metalloporphyrin rather than to changes in electronic coupling. The magnitude of the diminution is greater for the Mg-containing arrays, which is due to the greater driving force for charge separation. (5) The Zn-containing arrays are quite robust while the Mg-containing arrays are slightly labile toward demetallation and photooxidation. Taken together, these results indicate that porphyrin-based nanostructures having high energy-transfer efficiencies can be constructed from either Mg- or Zn-porphyrins. However, Mg-containing arrays may be superior in situations where a succession of energy-transfer steps occurs (due to a slightly higher yield per step) or where charge transfer is a desirable feature. On the other hand, Zn-porphyrins are better suited when it is desirable to avoid charge transfer quenching reactions. Accordingly, the merits of constructing a device from Mg- *vs.* Zn-containing porphyrins will be determined by the interplay of all of the above factors.

The ability to construct molecular systems with well defined three-dimensional architectures on the nanometre scale holds revolutionary potential for many disciplines, especially materials chemistry where macroscopic objects can be designed and constructed with molecular-level precision. Nanostructures designed for manipulation of optical phenomena are of particular interest for a variety of applications that are not possible with bulk materials. Some examples include the following. (1) Light-harvesting nanostructures can be used as energy funnels with applications in solar energy or as energy sources to power molecular devices. (2) Molecular photonic wires and gates can be used to transmit and manipulate signals in nanoscale information processing systems. (3) Structured composites of absorbers and emitters can serve as nanoscale optical sources or nanoscale imaging elements. All of these structures represent a broad class of photonic devices whose performance can be controlled in the nanoscale regime.

A major source of inspiration for the design and synthesis of optical nanostructures derives from the light-harvesting antenna complexes of natural photosynthetic systems. The antenna complexes are comprised of a large number of pigments that are arranged in a rigid three-dimensional matrix. The natural antenna complexes absorb light and funnel the resultant energy to the reaction centres *via* excited-state energy migration processes.[1] The energy migration process is extremely rapid (hopping time of *ca.* 0.1–1 ps per bacteriochlorophyll)[2] and has a quantum efficiency of nearly unity. Creating synthetic mimics of the natural antenna complexes has been a major objective of the field of artificial photosynthesis. More recently, such synthetic mimics have been tailored to serve as molecular photonic devices in materials chemistry.

The versatile optical (absorption and emission), redox, and photochemical properties of the porphyrins makes them ideally suited as components of nanostructures with optical features in the visible or near-IR spectral regions. Towards this goal, we have developed a modular building block synthesis of soluble multiporphyrin arrays comprised of metalloporphyrins or a composite of both metallo- and free-base porphyrins.[3–11] This building block approach has been used to construct a variety of molecular architectures containing from two to nine porphyrin constituents. The ability to construct successively more complicated, soluble molecular structures in a systematic fashion has permitted us to investigate the mechanisms and factors controlling electronic communication in the synthetic

multiporphyrin arrays, starting with the fundamental pairwise interactions characteristic of the dimeric systems. Our previous work on dimeric, trimeric, and star-shaped pentameric arrays has provided significant insights into the nature of these basic interactions.[12–15] The information garnered from our studies has been used as a guide for constructing prototypical molecular photonic wires[5] and optoelectronic gates[10] that utilize the multiporphyrin motif. Other workers have also developed routes to large covalently linked porphyrin arrays. Architectures prepared include star-shaped pentamers,[16–18] linear pentamers,[19] larger linear arrays up to nonamers,[20] three-dimensional nonamers,[18] polymeric arrays,[21] and self-assembled pentamers.[22] However, only a few of these routes enable precise specification of the metallation state of the various porphyrins in the array.

A key structural element common to all of our multiporphyrin arrays is a diarylethyne linker that joins the constituent porphyrins at the *meso*-carbon atom of the porphyrin macrocycles. The diarylethyne linkers are non-polar, establish a relatively fixed inter-porphyrin distance (*ca.* 20 Å centre-to-centre) albeit with free rotation about the ethyne in fluid solution,[15] and enable weak electronic interactions among the porphyrins.[12–14] These features of the molecular architecture promote extremely efficient (*ca.* 99%) energy transfer which predominantly involves a through-bond process mediated by the diarylethyne linker.[13] Our previous studies of dimeric arrays indicate that the rate of energy migration can be explicitly controlled by structural modification of the linker, specifically, *via* alteration of the substituent groups on the aryl rings. We anticipate that the rates of energy transfer would also be affected by other properties of the linker such as its effective length and geometry. Another important design element for controlling the physico-chemical properties of the multiporphyrin arrays is the selection of the metal ion in the metalloporphyrin. The metal ion modulates the redox potential,[23] conformation,[24] and excited-state lifetime[25] of the metalloporphyrin constituent and hence, could affect the electronic communication in the arrays.

Studies in the field of artificial photosynthesis ultimately require a molecular species which plays the role of (bacterio)-chlorophyll. Although (bacterio)chlorophyll contains a central magnesium ion, most studies in artificial photosynthesis have employed Zn- rather than Mg-complexes.[26] Relatively few model systems containing Mg-porphyrins have been prepared, and these have involved porphyrin monomers,[27] dimers,[28] trimers,[29] and larger aggregates of non-covalently linked porphyrins.[30] The dearth of artificial photosynthetic systems containing Mg-complexes originates mainly in historic synthetic difficulties in preparing Mg-porphyrins. Although Mg- and Zn-porphyrins have grossly similar features, Mg-porphyrins have four- to five-fold larger fluorescence yields ($W_f = 0.15$),[31] four- to five-fold longer fluorescence lifetimes ($t = 8$–10 ns),[31] and 100–300 mV lower oxidation potentials.[10,23,32] The photochemical consequences of these distinctions between Mg- and Zn-porphyrins, particularly with regards to energy- and/or electron-transfer reactions, remain largely unexplored. Probing these distinctions is essential not only for understanding artificial photosynthetic models but also for the rational design of molecular devices that transcend photosynthesis, such as molecular optoelectronic gates where a Zn-porphyrin provides for energy transfer and a Mg-porphyrin functions as a redox switch.[10]

Recently, we developed two simple methods for the preparation of Mg-porphyrins.[33,34] The removal of this synthetic obstacle affords an opportunity for systematically exploring the physico-chemical properties of these systems. In this paper, we combine the new synthesis of Mg-porphyrins with the building block synthesis of multiporphyrin arrays. These methods are used to prepare a series of dimeric and star-shaped pentameric arrays containing Mg-porphyrins, and an identical set comprised of Zn-porphyrins (Fig. 1). These arrays are structurally analogous to a series of previously studied Zn-porphyrin systems.[4,6,12] The dimers and star-shaped pentamers have dimensions along the porphyrin–diphenylethyne framework of *ca.* 4 and 6 nm, respectively. The availability of both sets of arrays enables a direct comparison of the synthesis, purification, chemical characterization, and spectroscopic properties of multiporphyrin arrays comprised of Mg- *vs.* Zn-porphyrins. Inasmuch as Zn-porphyrins are four- or five-coordinate depending on the solvent, while Mg-porphyrins are five- or six-coordinate, the new arrays provide the opportunity to investigate the effects of solvent and metal coordination state on the photodynamics of energy transfer.

Experimental

Synthetic procedures

General. ^{1}H NMR spectra (300 MHz, IBM FT-300, GN 300), absorption spectra (HP 8451A, Cary 3), fluorescence spectra (Spex Fluoromax) and electrochemical data[12] were collected routinely. Mass spectra were obtained by laser-desorption mass spectrometry.[11] Toluene (Fisher, certified ACS) and THF (Fisher, certified) were distilled from $LiAlH_4$. CH_2Cl_2 (Fisher, certified ACS) was distilled from K_2CO_3. Triethylamine (Fluka, puriss) was distilled from CaH_2. All reagents were obtained from Aldrich. TLC plates were purchased from Baker (Baker-flex, aluminium oxide IB-F). Column chromatography was performed using silica (Baker flash silica), alumina (Fisher A540, 80–200 mesh) or various grades of deactivated alumina. Chromatography of porphyrins was performed with shielding from ambient light. The isolated yields of Mg- or Zn-porphyrins do not take into account any ligands on the metal ion. The Fb-porphyrin building blocks FbU, FbU′, FbU-I, FbU-I_4, and FbU-core have been prepared previously,[3] as have the Zn-porphyrin building blocks ZnU and ZnU′ (Fig. 1).[6]

Preparation of alumina with various activities. Deactivated alumina of various grades was prepared for use in column chromatography. To a sample of alumina (Fisher, A540, 80–200 mesh, grade I) in an open beaker was added deionized water dropwise *via* a pipette under vigorous mechanical stirring, after which stirring was continued for 1 h to ensure homogeneity. In this manner alumina with 9% w/w water, 12% w/w water, 15% w/w water (grade V), or 20% w/w water was prepared.[35]

Analytical size exclusion chromatography (SEC). The methods employed for analytical SEC have been described in detail.[6,9] Briefly, analytical SEC columns (styrene–divinylbenzene copolymer) were purchased from Hewlett Packard and Phenomonex. Analytical SEC was performed with a Hewlett-Packard 1090 HPLC using 500 Å (300×7.8 mm), 500 Å (300×7.5 mm) and 100 Å (300×7.5 mm) columns (5 mm) in series eluting with THF (flow rate = 0.8 ml min^{-1}; void volume *ca.* 14.4 ml). Reaction monitoring was performed by removing *ca.* 5 ml aliquots from the reaction mixture, diluting with 500 ml toluene (Fisher, certified ACS) and injecting 50 ml to the HPLC. Sample detection was achieved by absorption spectroscopy using a diode array detector with quantitation at 420 nm ($\pm$10 nm bandwidth, reference wavelength 475 nm), which best captures the Soret bands of the porphyrins.

Magnesium 5,10,15-trimesityl-20-{4-[2-(trimethylsilyl)ethynyl]phenyl}porphyrin (MgU)

Magnesium insertion was accomplished using the heterogeneous method.[33] To a solution of FbU (220 mg, 0.263 mmol) in 25 ml CH_2Cl_2 was added *N*,*N*-diisopropylethylamine (DIEA) (1.1 ml, 5.26 mmol) and MgI_2 (731 mg, 2.63 mmol). The reaction mixture was stirred at room temperature. After

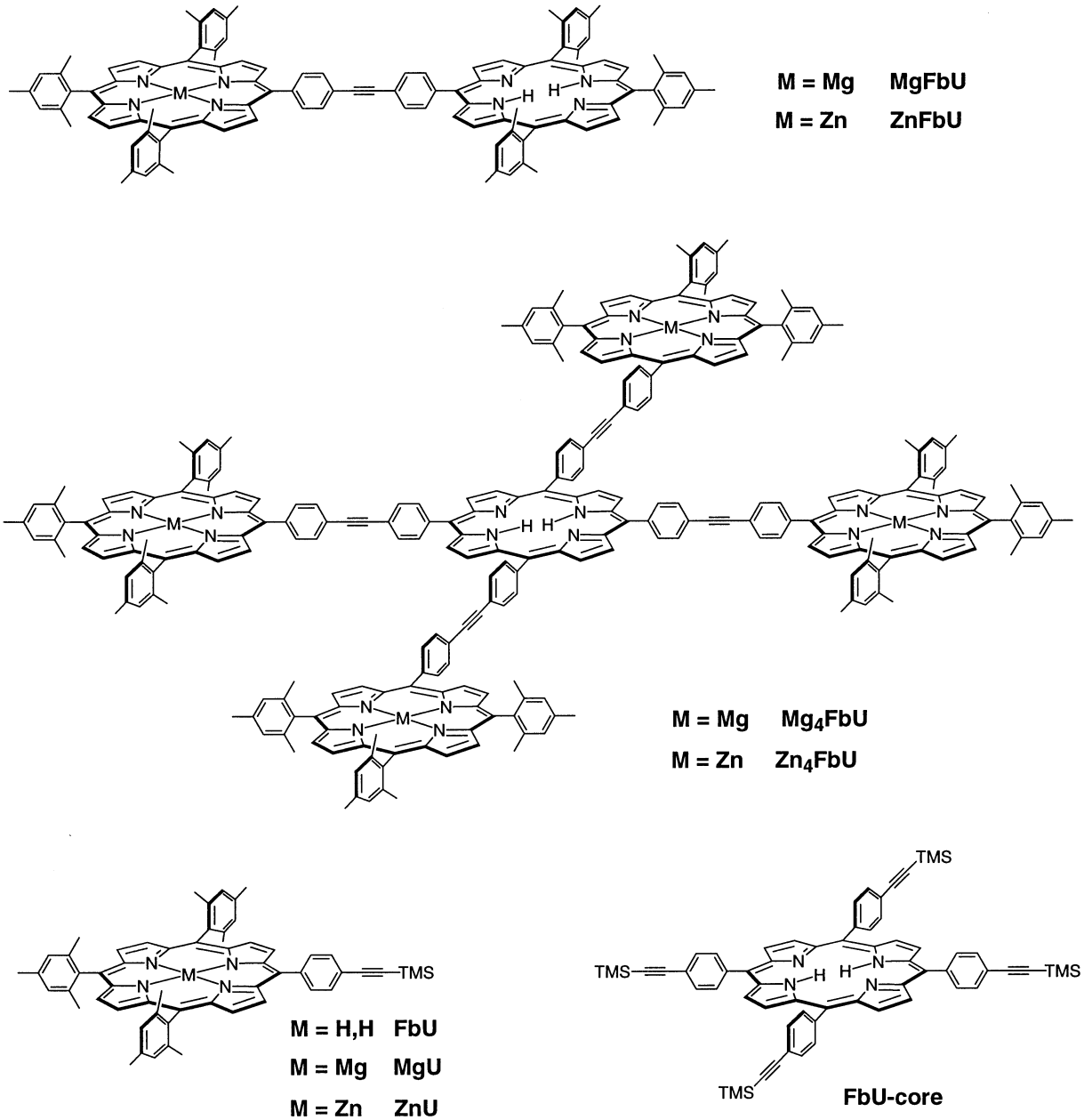

Fig. 1 Monomers, dimers and pentamers for spectroscopic study. Each compound has an unhindered, diphenylethyne linker, which is designated U for consistency with our previous nomenclature for related arrays.[13] The Zn-porphyrins are four- or five-coordinate, while the Mg-porphyrins are five- or six-coordinate (ligands are not shown) depending on the solvent. Although this diagram portrays the porphyrins in the arrays in coplanar geometries, in fluid solution at room temperature the porphyrins rotate freely about the ethyne, and the diphenylethyne linker bends slightly.[15] Replacement of the TMS-group with H in FbU, MgU, and ZnU affords FbU′, MgU′, and ZnU′.

30 min the reaction was judged to be complete by fluorescence excitation spectroscopy. The reaction mixture was diluted with 30 ml CH_2Cl_2, washed with 10% $NaHCO_3$ (2×50 ml), dried (Na_2SO_4), filtered, concentrated and chromatographed [Fisher A540 alumina, toluene–acetone (10:1), 3.8×5 cm] affording 223 mg (99% yield). ^{1}H NMR ($CDCl_3$) d 0.36 (s, 9 H, $SiCH_3$), 1.81 (s, 18 H, ArCH_3), 2.61 (s, 9 H, ArCH_3), 7.82 (AA′BB′, 2 H, ArH), 8.14 (AA′BB′, 2 H, ArH), 8.59–8.70 (m, 8 H, b-pyrrole); $C_{58}H_{54}MgN_4Si$ calc. av. mass 859.5u, obs. *m/z* 859.4; l_{abs} (toluene) 406(sh), 426, 566, 606 nm.

Magnesium 5,10,15-trimesityl-20-(4-ethynylphenyl)porphyrin (MgU′)

A solution of MgU (200 mg, 0.233 mmol) in 30 ml THF was treated with tetrabutylammonium fluoride (TBAF) on silica (373 mg, 1.0–1.5 mmol F g^{-1}) and the reaction was allowed to proceed for 60 min at room temperature. The reaction mixture was diluted with 30 ml ethyl acetate, extracted with 5% $NaHCO_3$ (2×50 ml) and water (2×50 ml) and then the organic layer was dried (Na_2SO_4). Column chromatography [Fisher A540 alumina, toluene–acetone (10:1), 3.8×5 cm] afforded 175 mg (95%). ^{1}H NMR ($CDCl_3$) d 1.82 (s, 12 H, ArCH_3), 1.87 (s, 6 H, ArCH_3), 2.60 (s, 9 H, ArCH_3), 3.32 (s, 1 H, CCH), 7.82 (AA′BB′, 2 H, ArH), 8.16 (AA′BB′, 2 H, ArH), 8.59–8.72 (m, 8 H, b-pyrrole); $C_{55}H_{46}MgN_4$ calc. av. mass 787.3u, obs. *m/z* 787.0; l_{abs} (toluene) 406(sh), 426, 566, 606 nm.

4-(Magnesium 5,10,15-trimesityl-20-porphinyl)-4′-(5,10,15-trimesityl-20-porphinyl)-diphenylacetylene (MgFbU)

The Pd-mediated coupling reaction follows the general procedure established previously.[6,9] Samples of ethynyl porphyrin MgU′ (32.2 mg, 41 mmol) and free-base iodoporphyrin FbU-

I (29.5 mg, 34 mmol) were dissolved in 15 ml toluene–triethylamine (TEA) (5:1) in a 25 ml one-neck round-bottomed flask. The flask was heated to 35 °C and was fitted with a 15 cm reflux condenser through which a drawn glass pipette was mounted for deaeration with argon. The reaction vessel was deaerated with a high flow rate of argon for 15 min. The tip of the pipette was then immersed in the solution. The argon flow rate was turned down and bubbling was continued for another 15 min. The condenser was then elevated, leaving the pipette tip in the solution, and Pd_2dba_3 (4.7 mg, 5.1 mmol) and $AsPh_3$ (12.5 mg, 41 mmol) were added to the mixture as solids simultaneously. The pipette was removed from the reaction mixture and positioned about 2 cm above the solution. The argon flow rate was turned up slightly and the reaction was allowed to proceed. After 2 h the reaction mixture was analysed by analytical SEC prior to concentration under reduced pressure. Analytical SEC showed a trace of material eluting at the leading edge of the product ($t_R < 24.4$ min), the product (t_R 25.4 min), and small amounts of monomeric porphyrin materials (t_R 27.5 and 28.2 min). TLC analysis [Baker alumina, toluene–acetone(15:1)] showed starting material FbU-I (R_f 0.9), a non-fluorescent component (R_f 0.6), MgFbU (R_f 0.5), MgU′ (R_f 0.3), and some baseline materials. The reaction mixture was dissolved in toluene and passed over an alumina (deactivated with 15% w/w water) column (3.8 × 5 cm) and eluted with toluene. $AsPh_3$ elutes rapidly, followed by a mixture of mobile porphyrins, and dark material including the Pd-reagents remains at the top of the column. The band consisting of MgFbU and trace amounts of high molecular mass materials and porphyrin monomers was collected. The mixture of porphyrins was concentrated, dissolved in toluene and loaded onto a preparative SEC column (BioRad Bio-Beads SX-1 in THF, 4.8 × 60 cm, gravity-flow, 4 ml min^{-1}). The high molecular mass material eluted first followed by the dimer MgFbU. Analytical SEC indicated that the dimer band contained trace amounts of high molecular mass material and monomeric porphyrin. The impure dimer was then chromatographed again on alumina as described for the first column. A faint yellowish band eluted quickly. The second band was collected and afforded MgFbU (38 mg) in 74% yield. ^{1}H NMR ($CDCl_3$) d −2.53 (br s, 2 H, NH), 1.87 (s, 24 H, ArCH_3), 2.44 (s, 18 H, ArCH_3), 2.64 (s, 12 H, ArCH_3), 7.28 (s, 8 H, ArH), 7.29 (s, 4 H, ArH), 8.02–8.08 (m, 4 H, ArH), 8.26–8.30 (m, 4H, ArH), 8.62–8.87 (m, 16 H, b-pyrrole); $C_{108}H_{92}MgN_8$, calc. av. mass 1526.3u, obs. *m/z* 1526.6; l_{abs} (toluene) 430, 516, 564, 604, 650 nm.

4-(Zinc 5,10,15-trimesityl-20-porphinyl)-4′-(5,10,15-trimesityl-20-porphinyl)-diphenylacetylene (ZnFbU)

Prepared previously.[6]

4-(5,10,15-Trimesityl-20-porphinyl)-4′-(5,10,15-trimesityl-20-porphinyl)-diphenylacetylene (Fb_2U)

Samples of ethynyl porphyrin FbU′ (19.9 mg, 26 mmol) and iodoporphyrin FbU-I (20.4 mg, 23.5 mmol) were coupled under similar conditions as described for MgFbU. Analytical SEC of the crude reaction mixture showed a trace amount of high molecular mass materials (t_R *ca.* 24.0 min), the product (t_R 25.5 min) and a small amount of monomeric porphyrin materials (t_R 28.3 min). TLC [silica, toluene–hexanes (3:2)] showed starting material FbU-I (R_f 0.74), Fb_2U (R_f 0.53) and some slow-moving materials ($R_f < 0.18$). No butadiyne-linked dimer[9] (R_f 0.59) was observed. Flash chromatography [silica, toluene–hexanes (3:2), 3.8 × 10 cm] afforded the product (28 mg, 79%). ^{1}H NMR ($CDCl_3$) d −2.56 (s, 4 H, NH), 1.85 (s, 36 H, *o*-ArCH_3), 2.61 (s, 18 H, *p*-ArCH_3), 7.26 (s, 12 H, ArH), 8.04 (AA′BB′, 4 H, ArH), 8.26 (AA′BB′, 4 H, ArH), 8.65,8.78 (m, 16 H, b-pyrrole); $C_{108}H_{94}N_8$ calc. av. mass 1503.9u, obs. *m/z* 1502.4; l_{abs} (toluene) 424, 516, 550, 594, 650 nm.

4-(Magnesium 5,10,15-trimesityl-20-porphinyl)-4′-(magnesium 5,10,15-trimesityl-20-porphinyl)diphenylacetylene (Mg_2U)

To a solution of Fb_2U (13.7 mg, 0.0091 mmol) in 1 ml CH_2Cl_2 was added *N*,*N*-diisopropylethylamine (32 ml, 0.182 mmol) and MgI_2 (25.5 mg, 0.091 mmol).[33] The reaction mixture was stirred at room temperature. After 30 min the reaction was judged to be complete by fluorescence excitation spectroscopy. The reaction mixture was diluted with 10 ml CH_2Cl_2, washed with 10% $NaHCO_3$ (2 × 10 ml), dried (Na_2SO_4), filtered, concentrated and passed over a column [Fisher alumina, toluene–acetone (10:1), 3.8 × 5 cm] affording 14 mg (99% yield). ^{1}H NMR ($CDCl_3$) d 1.85 (s, 24 H, ArCH_3), 2.38 (s, 18 H, ArCH_3), 2.62 (s, 12 H, ArCH_3), 7.24 (s, 12 H, ArH), 8.00 (AA′BB′, 4 H, ArH), 8.26 (AA′BB′, 4 H, ArH), 8.61–8.84 (m, 16 H, b-pyrrole); $C_{108}H_{90}Mg_2N_8$ calc. av. mass 1548.6u, obs. *m/z* 1547.0; l_{abs} (toluene) 406(sh), 426, 526, 566, 606 nm.

Mg_4FbU

In a 50 ml reaction vessel was added tetraiodoporphyrin FbU-I_4 (19.9 mg, 17.8 mmol) and 20 ml toluene–triethylamine (5:1). Sonication (Fisher sonicating bath, FS14) afforded complete dissolution of FbU-I_4, after which MgU′ (70 mg, 89.2 mmol) was added. The flask was immersed in an oil-bath at 35 °C and was equipped with a reflux condenser through which a drawn glass pipette was positioned for deaeration with argon. The reaction apparatus was deaerated with a high flow rate of argon for 15 min. The solution was then deaerated with the tip of the pipette immersed in the solution with gentle bubbling of argon for 15 min. Then the condenser was elevated and Pd_2dba_3 (9.8 mg, 10.7 mmol) and $AsPh_3$ (26.2 mg, 85.6 mmol) were added as solids simultaneously. The condenser was repositioned and argon bubbling was continued for 5 min. The pipette tip was then replaced about 2 cm above the solution and the argon flow rate was turned up slightly. The reaction course was monitored by analytical SEC. Aliquots (*ca.* 5 ml) were taken by a drawn glass capillary tube through the condenser in order to minimize admission of air into the reaction flask. After 2 h the reaction mixture consisted of a small amount of high molecular mass materials, a large amount of pentamer, small amounts of porphyrinic intermediates and unreacted MgU′. Additional Pd_2dba_3 (9.8 mg, 10.7 mmol) and $AsPh_3$ (26.2 mg, 85.6 mmol) were added. At 6.5 h, the reaction was judged to be complete. TLC analysis [Baker alumina, toluene–acetone (10:1)] showed the starting material MgU′ followed by a streak of fluorescent porphyrinic materials and some baseline materials. The crude mixture was concentrated to dryness, dissolved in toluene–$CHCl_3$ (3:2) and passed over a short column (3.8 × 5 cm) of alumina (deactivated with 15% w/w water) and eluted with toluene–$CHCl_3$ (3:2). The chromatography column was shielded with a black cloth. $AsPh_3$ eluted first followed by an intense band consisting of porphyrins. Some dark-coloured materials remained at the top of the column. The mixture of porphyrins was concentrated, dissolved in toluene and loaded onto a preparative SEC column (BioRad Bio-Beads SX-1 in THF, 4.8 × 60 cm, gravity-flow, 4 ml min^{-1}). The pentamer band was collected with small amounts of high molecular mass materials, tetrameric and trimeric porphyrin intermediates. The impure pentamer was rechromatographed by SEC in the same manner affording a mixture of the pentamer and trace amounts of higher molecular mass porphyrinic materials, and tetrameric and trimeric porphyrins. This mixture was then chromatographed on alumina (deactivated with 15% w/w water; column = 3.8 × 10 cm) with elution using toluene–$CHCl_3$(5:2). The third band was collected, affording 30 mg (45%) of pentamer Mg_4FbU. A final passage over the same preparative SEC column, with removal of the leading edge of the band (< 5% of total material) resulted in sharpening of the analytical SEC peak from FWHM = 0.71 to 0.65 min. ^{1}H NMR 500 MHz ($CDCl_3$) d −2.61 (s, 1 H, NH), 1.88 (s, 24

H, *o*-ArCH_3), 1.89 (s, 48 H, *o*-ArCH_3), 2.65 (s, 12 H, *p*-ArCH_3), 2.67 (s, 24 H, *p*- ArCH_3), 7.28 (s, 8 H, ArH), 7.31 (s, 16 H, ArH), 8.10 (AA′BB′, 8 H, ArH), 8.17 (AA′BB′, 8 H, ArH), 8.35–8.40 (m, 16 H, ArH), 8.65 (m, 16 H, b-pyrrole peripheral porphyrins), 8.76 (d, 8H, $J=4.4$ Hz, b-pyrrole peripheral porphyrins), 8.89 (d, 8H, $J=4.4$ Hz, b-pyrrole peripheral porphyrins), 9.07 (s, 8 H, b-pyrrole core porphyrin); $C_{264}H_{206}Mg_4N_{20}$ calc. av. mass 3755.9u, obs. *m/z* 3759.4; l_{abs} (toluene) 430, 522, 564, 606, 648 nm.

Zn_4FbU

Samples of FbU-I_4 (19.9 mg, 17.8 mmol) and ZnU′ (73.9 mg, 89.2 mmol) were coupled exactly as described for Mg_4FbU, and the product distribution observed by analytical SEC was identical with that of Mg_4FbU. The crude mixture was concentrated to dryness, dissolved in CH_2Cl_2 and passed over a short column of silica (CH_2Cl_2, 3.8×5 cm) shielded with a black cloth. $AsPh_3$ eluted first, followed by an intense band of porphyrins, with dark-coloured materials left at the top of the column. The mixture of porphyrins was concentrated, dissolved in toluene and loaded onto a preparative SEC column (BioRad Bio-Beads SX-1 in THF, 4.8×60 cm, gravity-flow, 4 ml min^{-1}). The pentamer band was collected with small amounts of high molecular mass materials, tetrameric and trimeric porphyrin intermediates. The impure pentamer was rechromatographed *via* SEC in the same manner affording a mixture of the pentamer and trace amounts of higher molecular mass porphyrinic materials, and tetrameric and trimeric porphyrins. This mixture was then chromatographed on silica (3.8×10 cm) using CH_2Cl_2–hexanes(3:2). The first band afforded 38 mg (55%) of pentamer Zn_4FbU. A final passage over the same preparative SEC column, with removal of the leading edge of the band (<5% of total material) resulted in sharpening of the analytical SEC peak from FWHM = 0.68 to 0.64 min. ^{1}H NMR 500 MHz ($CDCl_3$) d −2.60 (s, 2 H, NH), 1.90 (s, 72 H, *o*-ArCH_3), 2.62 (s, 12 H, *p*-ArCH_3), 2.65 (s, 24 H, *p*-ArCH_3), 7.31 (s, 8 H, ArH), 7.33 (s, 16 H, ArH), 8.13 (AA′BB′, 8 H, ArH), 8.18 (AA′BB′, 8 H, ArH), 8.36 (AA′BB′, 8 H, ArH), 8.40 (AA′BB′, 8 H, ArH), 8.75 (m, 16 H, b-pyrrole peripheral porphyrins), 8.85 (d, 8 H, $J=4.5$ Hz, b-pyrrole peripheral porphyrins), 8.98 (d, 8 H, $J=4.5$ Hz, b-pyrrole peripheral porphyrins), 9.08 (s, 8 H, b-pyrrole core porphyrin); $C_{264}H_{206}N_{20}Zn_4$ calc. av. mass 3920.2u, obs. *m/z* 3918.5; l_{abs}(toluene) 424, 429, 519, 551, 590, 651 nm.

Spectroscopic methods

Absorption and fluorescence spectroscopy. Absorption spectra were collected using a Varian Cary 3 with 1 nm bandwidths and 0.25 nm data intervals. Fluorescence spectra were collected using a Spex Fluoromax with 1 mm slit widths (4.25 nm) and 1 nm data intervals. Emission spectra were obtained with $A_{\lambda exc}<0.1$. Quantum yields were determined by ratioing integrated corrected emission spectra to MgTPP (0.15),[31] ZnTPP (0.030)[36] or TPP (0.11)[36] in toluene. Fluorescence quantum yield measurements in other solvents were corrected for refractive index differences relative to toluene.[37] Excitation spectra were not corrected. Measurements were made at room temperature without deaeration of samples. The solvent relative permittivities (e) at room temperature for various solvents are as follows: toluene (2.38), ethyl acetate (6.02), tetrahydrofuran (THF, 7.58), acetone (20.7), 2-nitrotoluene (27.4), acetonitrile (37.5), dimethyl sulfoxide (DMSO, 46.7).[38]

Resonance Raman spectroscopy. Resonance Raman (RR) spectra were recorded with a triple spectrograph (Spex 1877) equipped with either a 1200 or 2400 groove mm^{-1} holographically etched grating in the third stage. A liquid-nitrogen-cooled, UV-enhanced 1152X298 pixel charge coupled device (Princeton Instruments, LN/CCD equipped with an EEV1152-UV chip) was used as the detector. All RR experiments were conducted at ambient temperature on samples dissolved in rigorously degassed HPLC grade or spectroscopic grade solvents (toluene, 2-nitrotoluene, CH_2Cl_2, DMF, or THF). The sample concentration was typically 0.05 mM. The sample solutions were contained in spinning 5 mm quartz NMR tubes. Spinning was found to be essential in order to prevent photodecomposition of the Mg-porphyrins. The excitation wavelengths were provided by the output of an Ar ion (Coherent Innova 400–15UV) laser. The Raman shifts were calibrated by using the known values of indene, fenchone and acetonitrile. The Raman shifts are accurate to ±1 cm^{-1} for strong and/or isolated bands. The laser power at the sample was typically 5–7 mW and the spectral resolution was *ca.* 2 cm^{-1} at a Raman shift of 1600 cm^{-1}.

Time-resolved absorption and fluorescence spectroscopy. Fluorescence lifetimes were acquired on an apparatus having a time response of *ca.* 0.5 ns. Samples (*ca.* 50 mM) in 1 cm cuvettes were degassed on a vacuum line. Excitation flashes at 532 nm having a duration of 30 ps were obtained by frequency doubling the output of an actively/passively mode-locked Nd:YAG laser operating at 7 Hz. The flashes had an energy of 0.5 mJ and were focused to 3 mm at the sample. Emission at 90° from the excitation path was collected by a lens, transmitted through a long-pass filter (Schott OG570 for metalloporphyrin emission or OG630 for Fb-porphyrin emission) and focused on a pin photodiode (Newport Research 818-BB-21 PIN). The output of the photodiode was connected directly to the input of a Tektronix 7912AD transient digitizer that was controlled by a personal computer. Typically 64 traces were averaged to obtain a fluorescence decay profile.

Transient absorption data were acquired as described elsewhere.[39] Samples in 2 mm pathlength cuvettes had a concentration of *ca.* 10 mM for measurements in the 410–560 nm region and a concentration of *ca.* 100 mM for measurements in the 600–750 nm region. The samples were excited with flashes at 582 nm having a duration of 0.2 ps. The flashes had an energy of 100 mJ and were focused to 1.5 mm at the sample. The absorption changes were probed with weak white-light (400–1000 nm) pulses also having a duration of *ca.* 0.2 ps. Absorption changes over a 150 nm wavelength span were acquired using a two-dimensional detection system. For each spectrum, data acquired with 300 flashes were averaged, giving a resolution in D*A* of ±0.005. Absorption changes were obtained as a function of time by sending the probe pulse down an optical delay line, which permitted pump–probe time delays of −300 ps to 3 ns.

Results

Synthesis of the building blocks and the arrays

Porphyrin building blocks. Monofunctionalized porphyrin building blocks were prepared *via* mixed aldehyde condensations. Lindsey and co-workers previously prepared the free-base trimesityl-monoethynylporphyrin (FbU) by condensing 4-[2-(trimethylsilyl)ethynyl]benzaldehyde and benzaldehyde with pyrrole,[3] but the separation of FbU from the mixture of six porphyrins was difficult. A more efficient separation method (Scheme 1) involves separation of the Zn- rather than the Fb-porphyrins.[6] In this method, the crude reaction mixture containing six porphyrins was chromatographed to remove non-porphyrinic materials. The mixture of six porphyrins was subjected to zinc-insertion conditions and column chromatography of the mixture of Zn-porphyrins readily afforded ZnU. After isolation, ZnU was demetallated with trifluoroacetic acid (TFA) in CH_2Cl_2 to afford the corresponding FbU. The magnesium chelate was prepared by treating FbU with MgI_2 and *N*,*N*-diisopropylethylamine in CH_2Cl_2 at room tempera-

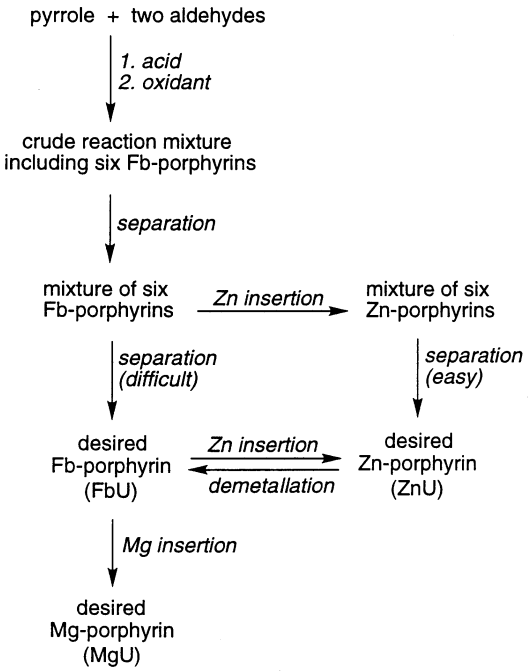

Scheme 1 Separation of FbU from the mixed condensation reaction mixture

ture with stirring for 30 min.[33] Column chromatography of the crude reaction mixture afforded MgU in 99% yield.

The trimethylsilyl group of MgU or ZnU was removed by treatment with TBAF on silica in THF at room temperature for 60 min (Scheme 2). No demetallation of either metalloporphyrin was observed during this reaction. ZnU′ was isolated by chromatography on silica.[3] However, due to the slightly acidic nature of silica, chromatography of MgU′ was performed on alumina in order to avoid demetallation. Both ZnU′ and MgU′ were isolated in 95% yield. In general, we have found that chromatography of the Zn-porphyrins could be performed on either silica or alumina, while Mg-porphyrins generally require chromatography on alumina rather than silica to avoid demetallation.

In pursuit of a direct route to MgU mirroring that used to isolate ZnU, we converted the mixture of Fb-porphyrins into Mg-porphyrins using the heterogeneous magnesium insertion

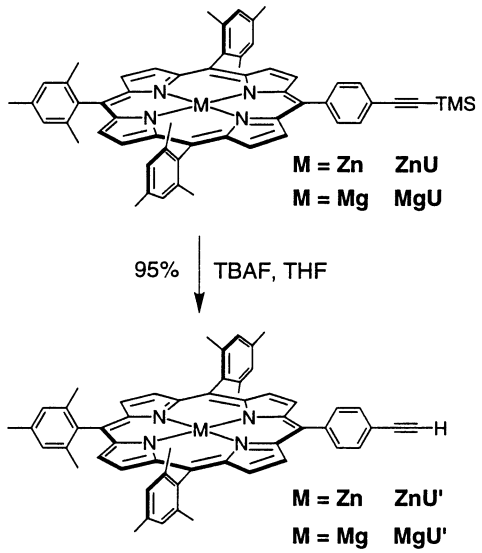

Scheme 2 Synthesis of porphyrin building blocks ZnU′ and MgU′

procedure. The attempted separation of MgU was carried out on alumina of various activities and with eluents of various polarities. Separation of the mixture of six Mg-porphyrins was achieved on alumina TLC [Baker alumina, toluene–$CHCl_3$ (20 : 1)]. However, column chromatography on alumina grade I or deactivated alumina containing 9, 15 or 20% water was ineffective in separating the porphyrins. Accordingly, the preferable route for forming MgU involves isolation of ZnU followed by demetallation and magnesium insertion. By this sequence, each of the metalloporphyrin building blocks (ZnU, MgU) was prepared in 200 mg quantities in *ca.* 2 days.

Trimesitylmonoiodoporphyrin (FbU-I) was prepared *via* condensation of 4-iodobenzaldehyde and mesitaldehyde with pyrrole as described previously.[3] In contrast to FbU, FbU-I was easily separated by column chromatography on silica.[3,6] The tetraiodoporphyrin FbU-I_4 was synthesized by condensation of 4-iodobenzaldehyde and pyrrole and was purified by column chromatography.[3]

Dimeric arrays. The key reaction for the synthesis of the arrays involves the Pd-catalysed coupling of an ethynylphenyl porphyrin and an iodophenyl porphyrin. We previously optimized this coupling reaction for the synthesis of multiporphyrin arrays containing Fb-porphyrins and Zn-porphyrins,[9] and used this method to prepare ZnFbU.[6] The optimization was performed in order to achieve good yields of the diarylethyne-linked porphyrin array under mild conditions in the absence of any copper cocatalysts, and to minimize formation of higher molecular mass byproducts as well as diarylbutadiyne-linked dimers. The optimized conditions enable the coupling to be performed with 1.5–5 mM of each porphyrin in toluene–triethylamine (5 : 1) in the presence of tris(dibenzylideneacetone) dipalladium(0) (Pd_2dba_3) and triphenylarsine ($AsPh_3$) under argon at 35 °C for 2 h. The molar ratio of the components is as follows: ethyne (1.25), iodide (1), Pd_2dba_3 (0.15), $AsPh_3$ (1.2). To establish the compatibility of Mg-porphyrins with these coupling conditions, magnesium tetraphenylporphyrin (MgTPP) was subjected to the same coupling reaction conditions. After 2 h, TLC and analytical SEC showed no decomposition, demetallation, or transmetallation of MgTPP. For the synthesis of porphyrin arrays, the reaction course is easily monitored by analytical size exclusion chromatography (SEC) coupled with a UV–VIS diode array detector. Chromatograms collected periodically provide a clear indication of product distribution over time.

The reaction of ethynylporphyrin MgU′ (2.73 mM) and iodoporphyrin FbU-I (2.27 mM) under the Pd-mediated coupling conditions (30 mol% Pd atom–iodide and 120 mol% $AsPh_3$–iodide) was performed under argon at 35 °C (Scheme 3). After 2 h, SEC analysis of the reaction mixture showed a trace amount of high molecular mass materials, dimer MgFbU, and a small amount of porphyrin monomers. TLC analysis [Baker alumina, toluene–acetone (15 : 1)] showed FbU-I (R_f 0.9), a non-fluorescent component (R_f 0.6), MgFbU (R_f 0.5), MgU′ (R_f 0.3), and some baseline materials. The reaction mixture was concentrated and chromatographed [toluene–acetone (15 : 1)] on a short column of deactivated alumina (15% water), which removed the Pd-reagents and $AsPh_3$ from the porphyrin components. Preparative size exclusion chromatography of the mixture of porphyrins afforded MgFbU and a trace amount of monomeric porphyrins. Subsequent chromatography on deactivated alumina (15% water) afforded MgFbU in 74% overall yield. Characterization of MgFbU was performed by TLC, analytical SEC, ^1H NMR spectroscopy, absorption and fluorescence spectroscopy, and laser desorption mass spectrometry.

In an early attempt to synthesize MgFbU, we sought to insert magnesium selectively into the core of one porphyrin unit in the all-free-base dimer, Fb_2U. Fb_2U was prepared *via* the Pd-catalysed coupling reaction of ethynyl porphyrin FbU′

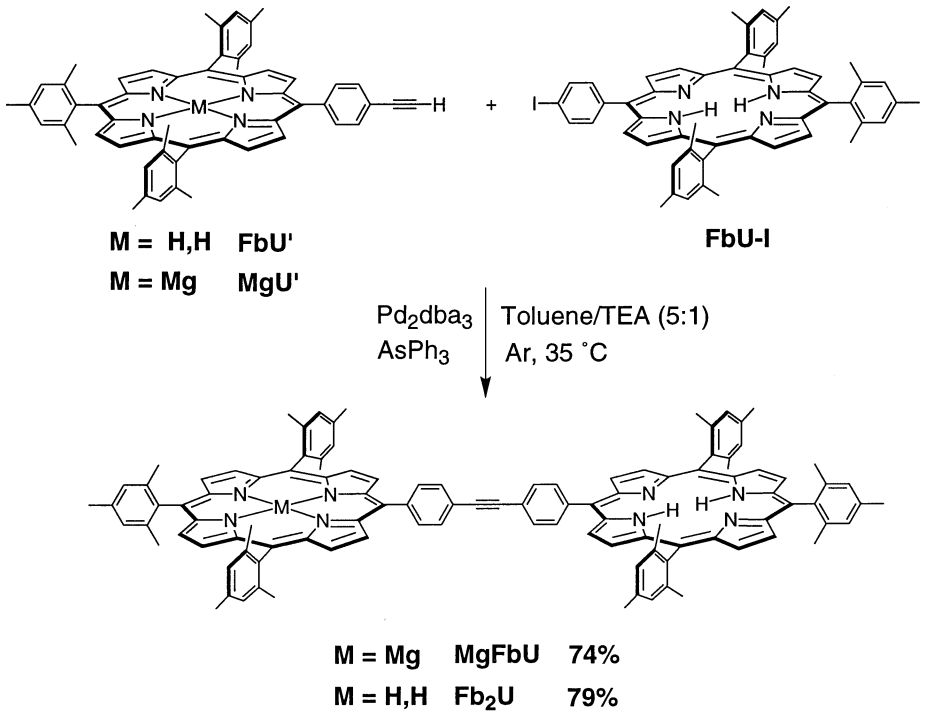

Scheme 3 Formation of dimeric arrays MgFbU and Fb_2U

and iodo porphyrin FbU-I, and was isolated in 79% yield after one flash silica chromatography column. Upon treatment of Fb_2U with MgI_2 (2–8 equiv.) and DIEA (4–16 equiv.) in CH_2Cl_2, no metallation was observed, while exposure to 10 equiv. MgI_2 and 20 equiv. DIEA afforded the completely metallated Mg_2U. These experiments aimed at selective metal insertion in a preformed array comprised of Fb-porphyrins proved ineffective in yielding the monomagnesiated dimer. In contrast, the desired MgFbU dimer is easily prepared by the rational coupling of Fb-porphyrin and Mg-porphyrin building blocks.

Star-shaped pentameric arrays. Previously we prepared two star-shaped Zn_4Fb-pentamers bearing 2,6-dimethoxyphenyl units or mesityl groups at the non-linked *meso*-positions. This synthetic work was done prior to the investigation of optimized Pd-coupling methods and before we had refined the chromatographic separation methods for these compounds. The diphenylethyne-linked pentamer bearing 2,6-dimethoxyphenyl groups was prepared by a coupling reaction at 100 °C for 12 h (45.6 mg, 45% isolated yield),[4,6] while a diphenylethyne-linked pentamer bearing mesityl groups was prepared by a coupling at 50 °C for two weeks (8.8 mg, 5.5% isolated yield).[40] For solubility reasons we have since focused on the mesityl-substituted arrays.[6] We now report a refined synthesis of a diphenylethyne-linked pentamer (Zn_4FbU), extend this route to the synthesis of a Mg_4FbU pentamer, and develop improved separation methods for isolating the pentamers.

The precursor to the core of the pentameric arrays, tetraiodoporphyrin FbU-I_4, has limited solubility in the coupling solvent toluene–triethylamine(5 : 1). To facilitate formation of the pentamer, we sought to keep the porphyrin concentrations as high as possible while maintaining homogeneous solutions. We found that the concentration of FbU-I_4 can be raised to 0.9 mM by dissolution with the aid of sonication. Thus, the metalloethynylporphyrin (ZnU′ or MgU′) and tetraiodoporphyrin FbU-I_4 concentrations were kept at 4.5 mM (5 equiv.) and 0.9 mM, respectively. The Pd-mediated coupling reaction was performed similarly as for the dimer syntheses (Scheme 4).

In the synthesis of pentamer Zn_4FbU, SEC analysis at 3 h revealed that the reaction mixture consisted of pentamer, small amounts of high molecular mass material, intermediates (tetramer, trimer and dimer) and starting material ZnU′. Tetraiodoporphyrin FbU-I_4 was completely consumed. Another portion of catalyst and ligand was added, and after an additional 3 h, the formation of Zn_4FbU levelled off. The product distribution during the course of reaction is shown in Fig. 2. The peaks of the dimeric, trimeric and tetrameric materials are well separated (t_R differences >1 min). The peaks of the tetrameric, pentameric and high molecular mass materials are clearly present but are not well resolved. By visual inspection, the pentamer-forming reaction remained homogeneous at all times. The crude reaction mixture was chromatographed first on silica to remove Pd-reagents and $AsPh_3$, then on two SEC columns which afforded the pentamer with trace amounts of tetrameric and trimeric porphyrins, and finally on silica which afforded the purified Zn_4FbU (55% overall yield). We found that the FWHM of the peak obtained by analytical SEC afforded one measure of purity. A subsequent passage of Zn_4FbU over the preparative SEC column led to removal of only a trace amount of the leading edge of the band, but caused the peak in the analytical SEC to sharpen from 0.68 to 0.64 min. This material was used for spectroscopic studies.

In the preparation of Mg_4FbU, the coupling reaction of MgU′ and FbU-I_4 and the product distribution as determined by analytical SEC were indistinguishable from that in the synthesis of Zn_4FbU. However, the purification procedure involved successive chromatography columns of deactivated alumina, SEC, SEC, deactivated alumina, and SEC. The development of this chromatography sequence involved examination of alumina having various degrees of deactivation, and alumina containing 12% water was found to give the best separation. The chromatography of Mg_4FbU on deactivated alumina was often complicated by streaking during the prolonged elution. Nonetheless, deactivated alumina was more effective for these arrays than sugar and other mild chromatographic media, which have traditionally been employed for separation of chlorophylls.[41] The pentamer can be purified to a considerable extent solely by chromatography on alumina columns, but the use of successive columns with different

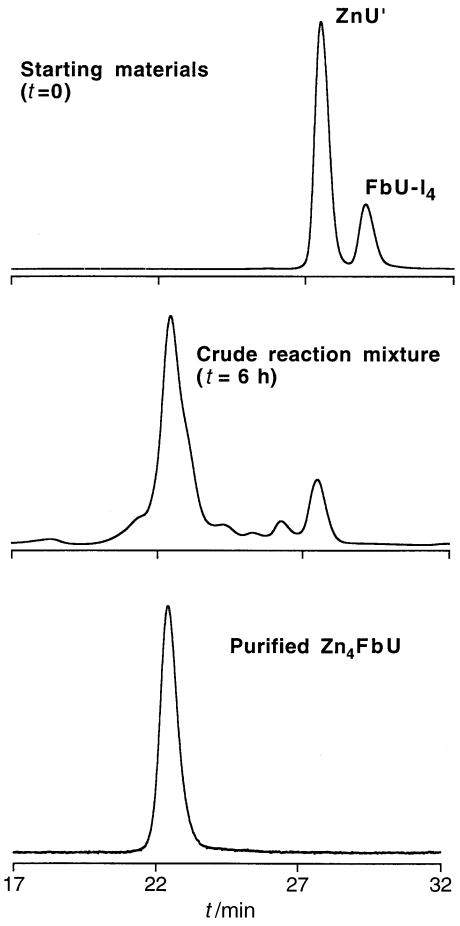

Fig. 2 Size exclusion chromatograms of the reaction forming Zn_4FbU pentamer. Top, starting materials (ZnU′ and FbU-I_4) before the catalyst was added. Middle, crude reaction mixture after 6 h. Bottom, purified Zn_4FbU pentamer. Identical chromatograms were observed for Mg_4FbU.

separation modalities provides the most effective purification procedure. The purified pentamer Mg_4FbU was isolated in 45% overall yield. In analogy with the Zn_4FbU pentamer, a subsequent passage of Mg_4FbU over the preparative SEC column led to removal of only a trace amount of the leading edge of the band, but caused the peak in the analytical SEC to sharpen from 0.71 to 0.65 min. This material was used for spectroscopic studies.

Chemical characterization and physical properties of the arrays

Purity. Each array (MgFbU, ZnFbU, Mg_4FbU, Zn_4FbU) was characterized by analytical SEC, ^{1}H NMR spectroscopy, laser desorption mass spectrometry, and absorption and fluorescence spectroscopy. Mass spectrometry indicates that there is no demetallation or transmetallation during the conversion of the porphyrin building blocks into the arrays. Discerning the presence of any impurities having lower molecular mass than the molecule ion is difficult due to fragmentation of the molecule ion. However, higher molecular mass impurities are readily observed. In the mass spectrum of Mg_4FbU a strong molecule ion was observed at m/z 3759.4, and in addition a much weaker peak was observed at m/z 4549.6. The latter is consistent with a hexamer comprised of five magnesium porphyrins and one free-base porphyrin. Similarly in the spectrum of the Zn_4FbU pentamer, a strong molecule ion was observed at m/z 3918.5 and a much weaker peak was observed at m/z 4750.0. The latter is consistent with a hexamer comprised of five zinc porphyrins and one free-base porphyrin. In each case the putative hexamer peak intensity was $\leqslant 5\%$ of that of the molecule ion peak. These higher mass peaks were observed in both laser desorption mass spectrometry (neat samples) and in matrix-assisted laser desorption mass spectrometry.[11] We believe these peaks to be synthesis byproducts, not mass spectrometric artifacts, although such impurities were not detected by analytical SEC. Based on these mass spectral peak intensities, and the amount of residual fluorescence emanating from the metalloporphyrins in the arrays, we estimate the purity of each pentameric array to be $\geqslant 95\%$. The dimers are estimated to be $\geqslant 97\%$ pure.

NMR features. The porphyrin building blocks and arrays were readily characterized by ^{1}H NMR spectroscopy at 300 or 500 MHz at room temperature in $CDCl_3$ at *ca.* 5 mM (monomers and dimers) or *ca.* 1 mM (pentamers) concentration. Upon formation of the arrays, the resonances from the b-pyrrole protons and from the protons flanking the ethynyl-unit exhibit characteristic features. For example, upon coupling of MgU′ and FbU-I to form MgFbU, the observed splitting pattern of the b-pyrrole protons is the sum of the splitting pattern of each of the component parts. The signals from the aryl protons flanking the ethyne linkage in the dimers shift downfield by *ca.* 0.2 ppm compared with the monomers. The changes in splitting pattern and chemical shift are similar to those previously reported for ZnFbU.[6] The pentameric arrays (Mg_4FbU and Zn_4FbU) exhibited similar spectral features in comparison with their respective monomeric precursors. A key diagnostic in the star-shaped pentamers is the singlet at d *ca.* 9 originating from the b-pyrrole protons of the core Fb-porphyrin, which has four-fold symmetry (assuming rapid N—H tautomerism). The chemical shifts of the respective protons in Mg_4FbU and Zn_4FbU differ by <0.2 ppm. However, the peaks of Mg_4FbU, particularly in the aromatic region, are slightly broader than those of Zn_4FbU. The line broadening observed with Mg_4FbU may be caused by the various accessible coordination states and ligands of the magnesium in the peripheral porphyrins. At higher concentration (*ca.* 5 mM), samples of Mg_4FbU and Zn_4FbU exhibit severe line broadening in the spectra, a sign of aggregation.

Solubility. For easy purification and characterization, high solubility of the arrays in various solvents is essential. The operational solubilities we have observed during the course of handling these compounds are listed in Table 1. These are not necessarily upper solubility limits. In addition, the dimers and pentamers are soluble in dilute solution in a wide range of solvents. For example, analytical SEC is performed in THF (10^{-5}–10^{-4} M), and absorption and fluorescence spectroscopy has been performed at $\leqslant 20$ mM in solvents such as ethyl acetate, acetone, acetonitrile and DMSO.

Chemical stability. In our routine handling of Mg-porphyrin-based arrays, we did not observe any decomposition or demetallation of solid samples stored at room temperature in the dark over a period of 1–2 weeks. The Mg-porphyrin containing arrays remain intact at $-5\,^{\circ}$C for *ca.* 3 months. The Mg-porphyrin monomers could be stored at $-5\,^{\circ}$C for longer periods, indicating their greater stability compared with the corresponding arrays. TLC analysis provided an effective assay for small amounts of decomposition of the Mg-porphyrin arrays. In particular, a fast-moving greyish-blue decomposition component was observed on alumina TLC. The solution absorption spectra of such samples also exhibited slight changes in the relative intensities of the Q bands. Samples of Mg-porphyrin arrays that exhibited any signs of deterioration were passed over a short column of deactivated alumina, which readily removed the mobile greyish-blue decomposition product(s). During synthesis and characterization, all Mg-porphyrins were protected against unnecessary exposure to

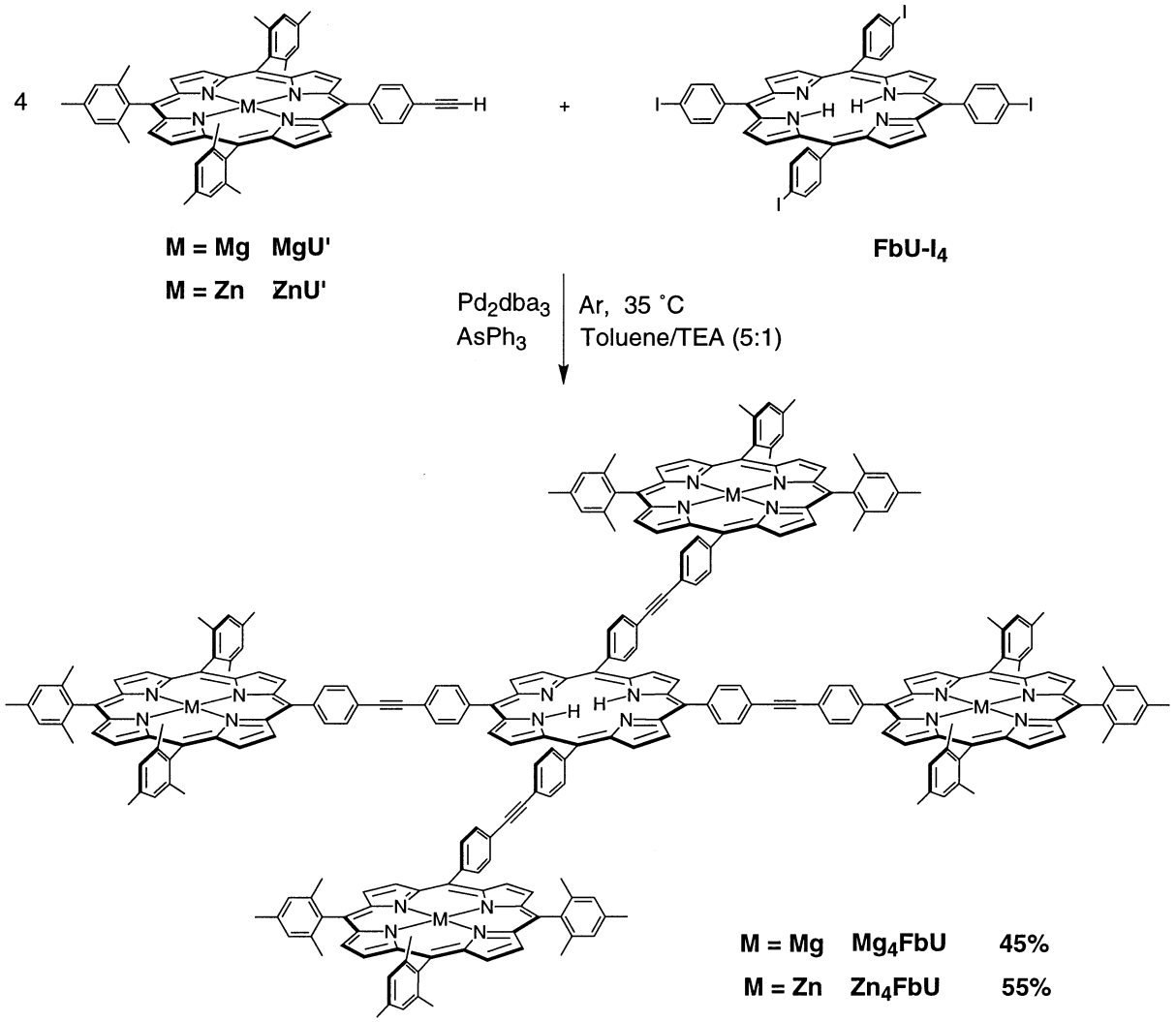

Scheme 4 Building block approach in the synthesis of pentamers Mg_4FbU and Zn_4FbU

air and light. In contrast to the Mg-porphyrin arrays, the Zn-porphyrin arrays appear to be stable indefinitely when stored in solid form at $-5\,^{\circ}C$.

Although the Mg-porphyrins and Mg-porphyrin-based arrays were sufficiently stable for routine handling and spectroscopic characterization, thoughts about future, more robust, arrays containing Mg-porphyrins prompted us to follow up an earlier observation concerning electronic effects on stability of Mg-porphyrinic compounds. We observed that Mg-phthalocyanines are more stable toward demetallation than Mg-porphyrins,[34] which can be attributed to electron withdrawal by the four *meso*-nitrogens in the former compounds. To investigate whether this phenomenon carried over to Mg-porphyrins bearing electron-withdrawing groups, we treated 2 mM solutions of MgTPP, magnesium tetramesitylporphyrin (MgTMP),[33] and magnesium tetrakis(pentafluorophenyl)-porphyrin (MgPFPP)[34] in CH_2Cl_2 with acetic acid (0.3 M) at room temperature. After 1 h, MgTPP and MgTMP were demetallated quantitatively, while MgPFPP exhibited no demetallation after 24 h. This experiment illustrates the design principle that incorporation of electron-withdrawing groups provides enhanced stability of Mg-porphyrins toward demetallation.

Electrochemical properties. The redox potentials of the Zn- and Fb-porphyrins have been previously reported.[12,14] For these arrays the redox potentials of the constituent porphyrins are identical to those of the monomers. This is also the case for the components of MgFbU and Mg_4FbU. It is noteworthy

Table 1 Operational solubilities (mM) of arrays

array	toluene–TEA (5:1)[a]	chromatography solvent[b]	toluene[c]	$CDCl_3$[d]
Fb_2U[e]	5.8	5–8[f]		8
MgFbU	2.3	5–7[g]	10	8
Mg_4FbU	1	2.5[h]	2.5	3
Zn_4FbU	1	2.5[i]	2.5	5

[a]Solvent for Pd-mediated coupling reactions. [b]Solvent for adsorption chromatography (silica or deactivated alumina). [c]SEC loading solvent. [d]NMR solvent. [e]The solvent for magnesium insertion is CH_2Cl_2 in which the solubility is 9.1 mM. [f]Toluene–hexanes (3:2). [g]Toluene-acetone (15:1).[h]Toluene–$CHCl_3$ (3:1). [i]CH_2Cl_2–hexanes (3:2).

Table 2 Absorption maxima in various solvents (298 K)

	toluene (FWHM)	ethyl acetate	THF (FWHM)	acetone	acetonitrile	DMSO
monomers						
TPP	419 (12.0)	415	417 (15.0)	414	413	419
	548	545	546	546	547	550
MgTPP	426 (12.5)	422	429 (11.0)	422	425	426
	563	562	570	562	565	564
ZnTPP	423 (11.2)	421	423 (11.2)	422	422	427
	550	552	555	554	555	560
FbU	420 (12.7)	420	418 (13.5)	415	414	419
	548	548	547	545	546	548
MgU	428 (12.5)	425	433 (12.7)	425	425	428
	565	564	573	565	565	565
ZnU	423 (12.9)	424	425 (10.0)	424	424	430
	550	554	556	555	558	562
FbU-core	424 (15.0)		420 (14.0)			
	555		550			
dimers						
MgFbU	430 (19.5)	428		427	427	431
	565	564		564	564	565
ZnFbU	426 (18.9)	426	426 (16.7)	426	426	431
	550	553	556	554	556	562
pentamers						
Mg_4FbU	431 (16.0)		433 (12.7)			
	522, 565, 604, 650		518, 574, 615, 648			
Zn_4FbU	424, 429 (20.0)		429 (15.0)			
	519, 551, 590, 651		516, 558, 597, 648			

that the Mg-porphyrin is *ca.* 300 mV easier to oxidize than the Zn-porphyrin.[10]

Spectroscopic and photochemical properties of the arrays

Absorption spectra. The absorption spectra of various porphyrins and the arrays were measured in toluene at room temperature (Table 2). A slight bathochromic shift in the Soret band (2 nm) and Q bands (2 nm) is observed with building block MgU compared to MgTPP. In MgFbU, the Soret band shows no splitting but the absorption band is slightly red shifted (l_{max} 430 nm, shoulder at 420 nm at *ca.* 75% height) and broadened (FWHM = 19.5 nm) compared with MgU (428 nm) and FbU (420 nm). However, the visible absorption bands are nearly the sum of the spectra of the Fb- and Mg-porphyrin components. Similarly for Mg_4FbU, a broadened and red-shifted Soret band (431 nm, FWHM = 16 nm) is observed compared with the model porphyrins MgU (428 nm) and FbU-core (424 nm), while the visible bands of Mg_4FbU (522, 565, 604 and 650 nm) are nearly a superposition of those of the building blocks. The spectra of ZnFbU in various solvents have been described previously.[6,13] The pentamer Zn_4FbU exhibits nearly identical absorption spectral features as Mg_4FbU, though the former exhibits a very slightly split Soret band (424, 429 nm).

The absorption spectra of selected compounds were also collected in several more polar solvents. For MgTPP, MgU and MgFbU, only a slight shift (1–3 nm) in the Soret band and the Q bands is observed in ethyl acetate, acetone, acetonitrile or DMSO compared with toluene (Table 2). In THF, however, Mg-porphyrins exhibit bathochromic shifts of *ca.* 8 nm and a two-fold increase in intensity of the Q(1,0) band, giving green solutions. The absorption spectral changes of Mg-porphyrins in THF are attributed to the binding of two axial THF molecules, yielding a six-coordinate geometry, consistent with the Raman data reported below. Mg-porphyrins are five-coordinate in non-coordinating solvents, where water presumably serves as the fifth ligand. In all solvents examined here with the exception of THF, the Mg-porphyrins are predominantly if not exclusively five-coordinate. The small spectral shift of the Mg-porphyrins in acetone, acetonitrile or DMSO is in contrast to their zinc counterparts, which exhibit bathochromic shifts of up to 10 nm in these polar solvents. The shifts observed for the Zn-porphyrins are attributed to solvent ligation which converts the zinc ion from a four- to a five-coordinate geometry. Regardless of the solvent, the spectrum in the Q-band region of a given array closely resembles the sum of the spectra of the component parts in the same solvent.

Fluorescence spectra and quantum yields. The fluorescence emission spectra of the dimers were measured in toluene. Illumination of MgFbU at 648 nm, where the Fb-porphyrin absorbs about 20 times more strongly than the Mg-porphyrin, results in typical Fb-porphyrin emission with quantum yield ($W_f = 0.13$) nearly identical with the monomeric Fb-porphyrins, FbU or TPP. Illumination of MgFbU at 565 nm, where the Mg-porphyrin absorbs about 11 times as intensely as the Fb-porphyrin, results in emission predominantly from the Fb-porphyrin. The Mg-porphyrin emission yield ($W_f = 0.009$) is diminished 17-fold compared with MgU. The fluorescence yield measurements of MgFbU are summarized in Table 3. ZnFbU, which we have characterized previously,[13] has nearly identical features to MgFbU, including $\geqslant$20-fold quenching of the Zn-porphyrin compared with ZnU and dominant emission from the Fb-porphyrin upon illumination at 550 nm, where the Zn-porphyrin absorbs 80% of the light. Measurement of the small amounts of residual metalloporphyrin fluorescence is not a reliable means of placing a bound on the energy-transfer efficiency, due to difficulties in quantitation arising from spectral overlap, and the presence of fluorescent impurities at the few percent level that become significant in comparison to the strongly quenched metalloporphyrin in the arrays.[13] In particular, the small but quantifiable metalloporphyrin emission in MgFbU (in contrast to the negligible metalloporphyrin emission in ZnFbU) is likely due to impurities at the $\leqslant$3% level. Fluorescence excitation spectra provide a better overall view of the yield of energy transfer in donor–acceptor systems.[42,43] Close matching of the fluorescence excitation spectrum and absorption spectrum through the Q bands ($l_{em} = 720$ nm) was observed for each array (MgFbU, ZnFbU, Mg_4FbU, Zn_4FbU) in toluene. These results indicate a high yield of energy transfer, as absorption by the metalloporphyrin contributes fully to the observed emission of the Fb-porphyrin.

The fluorescence properties of MgFbU were examined in several more polar solvents. Again, close matching of absorp-

Table 3 Fluorescence yields in various solvents (298 K)

	toluene	ethyl acetate	acetone	acetonitrile	DMSO
monomers					
FbU	0.12	0.13	0.13	0.13	0.15
MgU	0.16	0.20	0.20	0.19	—[a]
ZnU	0.034	0.041	0.041	0.063	0.051
FbU-core arrays	0.15				
MgFbU					
Fb(em)[b]	0.13	0.13	0.069	0.050	0.017
Mg(em)[c]	0.009	0.013	0.009	0.009	
ZnFbU					
Fb(em)[b]	0.13	0.11	0.14	0.072	0.065
Zn(em)[c]	$\leqslant$0.002	$\leqslant$0.002	$\leqslant$0.004	$\leqslant$0.004	$\leqslant$0.003
Mg_4FbU					
Fb(em)[b]	0.11				
Mg(em)[c]	0.010				
Zn_4FbU					
Fb(em)[b]	0.14				
Zn(em)[c]	$\leqslant$0.004				

[a]Aggregation prevented measurement. [b]The emission from the Fb-porphyrin (l_{exc} = 648 nm) was measured in the range 660–800 nm. The total emission from the Fb-porphyrin (620–800 nm) was then inferred assuming the Fb-porphyrin in the array has the same emission spectral profile as the Fb-porphyrin monomer, and these values are reported in this Table.[6] [c]The emission from the metalloporphyrin (l_{exc} = 550–555 nm for Zn-porphyrins and l_{exc} = 562–565 nm for Mg-porphyrins) was measured in the range 570–800 nm. The total emission from the metalloporphyrin was inferred by measurement of the emission intensity in the 570–620 nm region and assuming the metalloporphyrin in the array has the same emission spectral profile as the metalloporphyrin monomer.[6]

tion and excitation spectra was observed in all solvents, consistent with a high yield of energy transfer. However, illumination at 648 nm gave typical Fb-porphyrin emission in all solvents but the quantum yield of the Fb-porphyrin emission decreased steadily with increasing solvent polarity (Fig. 3). In contrast, the fluorescence yields of the Fb-porphyrin monomers (or the Mg-containing monomers) changed only slightly as a function of solvent polarity. Illumination of the Mg-porphyrin (563–565 nm) in MgFbU yields a constant high degree of quenching of the Mg-porphyrin emission in all solvents, though the relative amount of Fb-porphyrin emission declined as the solvent polarity increased. Qualitatively similar results were

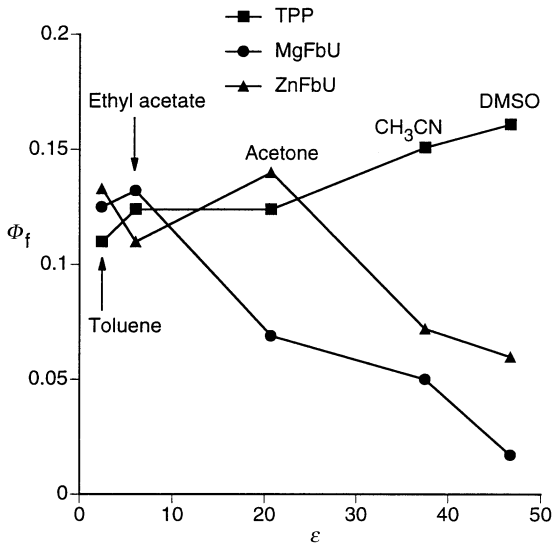

Fig. 3 Fluorescence quantum yield of TPP (&), and the Fb-porphyrins in MgFbU ($) and ZnFbU (+) measured by illumination at 648 nm as a function of solvent relative permittivity (corrected for solvent refractive index) at 298 K

obtained with ZnFbU, as noted earlier.[13] However, the magnitude of the decline in Fb-porphyrin fluorescence with increased solvent polarity was less than that with MgFbU (Fig. 3). Thus, MgFbU and ZnFbU exhibit high yields of energy transfer in all solvents but the emission from the Fb-porphyrin is quenched as the solvent polarity increases. The quenching of the excited-state Fb-porphyrin is attributed to charge transfer with the neighbouring ground-state metalloporphyrin following energy transfer.

Matched solutions of Mg_4FbU and of Zn_4FbU in toluene were illuminated at 565 nm, a wavelength where the two samples exhibit equal absorbance. The fluorescence emission spectrum of each sample was comprised predominantly of Fb-porphyrin emission. However, the Fb-porphyrin emission (measured in the range 625–800 nm) from Mg_4FbU was 13% less than that from Zn_4FbU. In addition, illumination of the Fb-porphyrin at 648 nm in Mg_4FbU and Zn_4FbU yielded W_f = 0.11 and 0.14, respectively (Table 3). These results indicate a slight amount of quenching of the Fb-porphyrin emission in Mg_4FbU compared with that of Zn_4FbU in toluene.

Resonance Raman spectra. The high-frequency regions of the B-state excitation (l_{exc} = 457.9 nm) RR spectra of ZnU, MgU, ZnFbU, and MgFbU in toluene are shown in Fig. 4 (left panel). The spectra obtained in 2-nitrotoluene are also shown in Fig. 4 (right panel). The key spectral features shown in the figure are the ethyne stretching mode, $n_{C\equiv C}$,[12] which is observed for the monomers at *ca.* 2156 cm^{-1} and for the dimers at *ca.* 2213 cm^{-1}, and the porphyrin skeletal mode, n_2, which is observed in the region 1543–1551 cm^{-1} for all the compounds.

Inspection of the RR data reveals that the frequencies of the

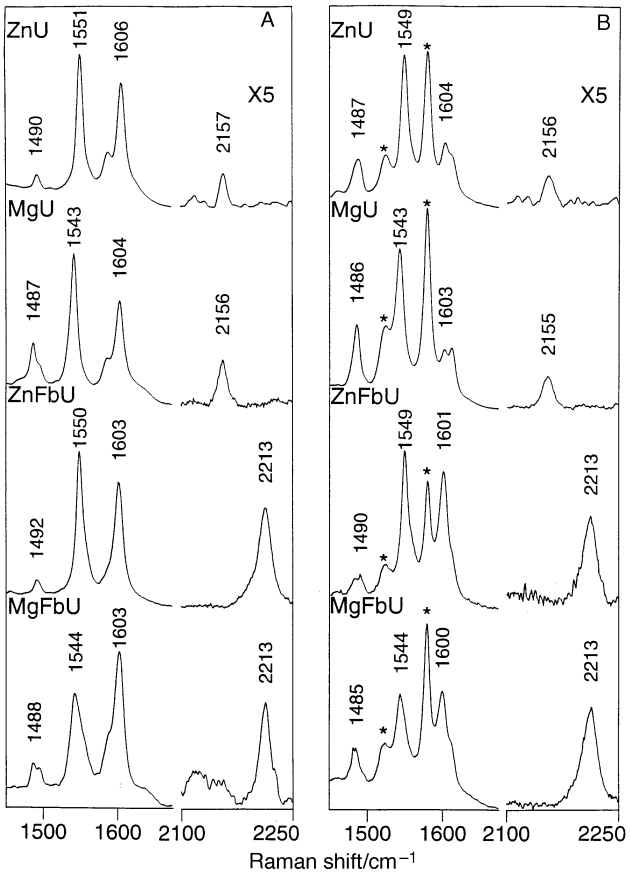

Fig. 4 The high-frequency regions of the B-state excitation (l_{exc} = 457.9 nm) RR spectra of ZnU, MgU, ZnFbU and MgFbU in toluene (A) and 2-nitrotoluene (B) obtained at 295 K. The bands marked by asterisks are due to solvent.

$n_{C=C}$ modes of MgU and ZnU are essentially identical. This is also the case for MgFbU and ZnFbU. On the other hand, the frequencies of the $n_{C=C}$ modes of the dimers are somewhat higher than those of the monomers. These differences are not due, however, to effects of linking the porphyrins in the array, but rather to the fact that the ethyne substituent of the monomers (FbU, ZnU, MgU) contains a terminal trimethylsilyl group rather than an appended aryl ring. In monomeric metalloporphyrins containing a diarylethyne substituent (MgU, ZnU), $n_{C=C}$ is at *ca.* 2217 cm^{-1},[12] nearly the same frequency observed for MgFbU and ZnFbU. The frequencies of the $n_{C=C}$ modes of the various Mg- and Zn-porphyrins are also identical in toluene and 2-nitrotoluene [and CH_2Cl_2, DMF, and THF (not shown)]. Together, these results indicate that the ground-electronic-state structure of the linkers is essentially identical in the Mg- and Zn-porphyrins and is not influenced by the properties of the solvent.

The RR spectra show that the frequencies of the n_2 modes of both MgU and MgFbU are lower than those of the Zn-containing analogues. These frequency differences are attributed to the fact that Mg- and Zn-porphyrins have slightly different structures and core geometries.[24] On the other hand, the frequencies of the n_2 modes of MgFbU and ZnFbU are approximately the same as those of MgU and ZnU, respectively, indicative of the fact that array formation does not affect the structure of the porphyrin ring(s).[12] The general appearance of the n_2 spectral features of MgFbU are, however, different from those of ZnFbU, whereas those of MgU and ZnU are quite similar. In particular, the n_2 feature of ZnFbU is relatively narrow and comparable in width to that of ZnU and MgU. On the other hand, the n_2 feature of MgFbU is somewhat broader and exhibits a shoulder on the high-frequency side. The narrowness of the n_2 feature of ZnFbU arises because the frequencies of the n_2 modes of the Zn- and Fb-components of the dimer are nearly coincident at *ca.* 1550 cm^{-1}. This was confirmed by RR data obtained for the free-base monomer (not shown). The slightly downshifted frequency of the n_2 mode of the Mg-component of MgFbU reveals the n_2 band of the Fb-component which remains at *ca.* 1550 cm^{-1}. The frequencies of the n_2 modes of ZnU and ZnFbU are nearly the same in toluene and 2-nitrotoluene [and CH_2Cl_2, THF and DMF (not shown)]. This is also the case for MgU and MgFbU in all solvents with the exception of THF. Accordingly, the ground-electronic-state structures of the porphyrin ring(s) are relatively insensitive to the dielectric properties of the solvent. In the case of the Mg-porphyrins in THF, the n_2 modes are downshifted to *ca.* 1536 cm^{-1} (not shown). This frequency shift is attributed to the fact that the Mg-porphyrin is hexacoordinate in THF, commensurate with the different absorption spectra observed in this solvent (*vide supra*).

Further inspection of the RR data reveals that the relative intensities of the $n_{C=C}$ *vs.* n_2 modes are approximately the same for the Mg- and Zn-porphyrins. In addition, these relative intensities remain the same in all of the solvents investigated (toluene, 2-nitrotoluene, CH_2Cl_2, THF and DMF). The increased relative intensities of the $n_{C=C}$ *vs.* n_2 modes of the dimers *vs.* monomers again arises because of the presence of terminal aryl *vs.* trimethylsilyl groups in the two systems (rather than being an effect of covalent linkage in the array).[12] The apparent increased relative intensity of the $n_{C=C}$ *vs.* n_2 mode of MgFbU *vs.* ZnFbU is solely due to the fact that the n_2 feature of the former dimer is broader than that of the latter. Integration of the RR band contours for MgFbU and ZnFbU reveals that the relative intensities of the $n_{C=C}$ *vs.* n_2 modes of the two different arrays are in fact identical. Collectively, these results indicate that the excited-state electronic coupling between the ethyne group and the p system of the porphyrin ring (which dictates the relative intensities of the $n_{C=C}$ *vs.* n_2 modes[12,14]) is similar in the Mg- and Zn-porphyrins and is not strongly influenced by the coordination of the metal ion or the dielectric properties of the solvent.

Time-resolved absorption spectra. The energy-transfer dynamics from the excited metalloporphyrin to the ground-state Fb-porphyrin in the ZnFbU and MgFbU dimers was probed using femtosecond transient absorption spectroscopy. Representative data for MgFbU and ZnFbU are shown in Fig. 5. The use of 582 nm pump flashes results in absorption by both the metalloporphyrin and Fb-porphyrin. Therefore, the transient absorption difference spectra immediately after excitation contain mixtures in which either the metalloporphyrin of the dimer is excited or the Fb-porphyrin is excited. This fact is revealed by the 1 ps spectrum for MgFbU in toluene shown in Fig. 5A. Although there are differences in peak positions and intensities, the singlet excited states of both the Mg- and Fb-porphyrins exhibit strong absorption between 430 and 500 nm corresponding to the Soret band of the excited state.[44] The dip near 515 nm in the 1 ps spectrum is due to bleaching of the shortest wavelength of the four ground-state Q bands of the Fb-porphyrin, namely the $Q_y(1,0)$ band. The dip near 560 nm is mostly due to bleaching of the Q(0,0) ground-state absorption band of the Mg-porphyrin, along with some Fb-porphyrin bleaching. The trough at 610 nm is comprised of Q(0,0) bleaching and stimulated emission from the Mg-porphyrin along with some bleaching of the $Q_x(1,0)$ band of the Fb-porphyrin. The dip near 650 nm also has overlapping contributions, namely $Q_x(0,0)$ bleaching and stimulated emission from the Fb-porphyrin and Q(0,1) stimulated emission from the Mg-porphyrin. Finally, the dip near 720 nm is due

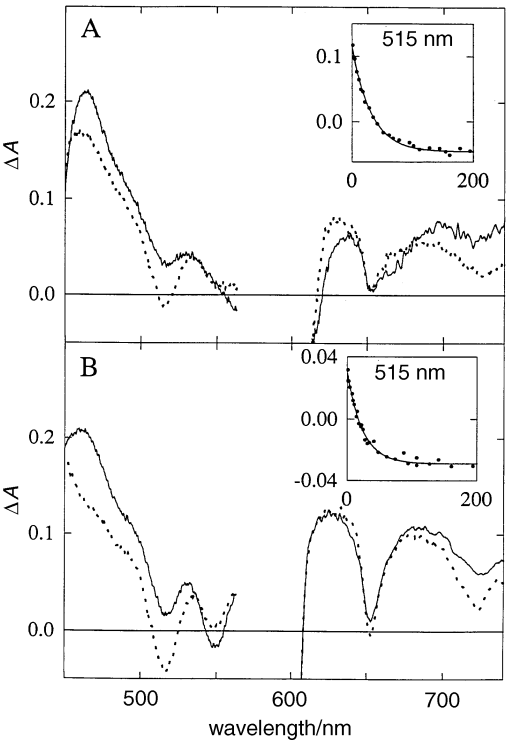

Fig. 5 Room-temperature transient difference spectra acquired following excitation of the dimers in toluene with a 0.2 ps flash at 582 nm. The spectra for MgFbU in (A) were acquired at time delays of 1 ps (solid) and 100 ps (dashed). The spectra for ZnFbU in (B) were acquired at time delays of 1 ps (solid) and 100 ps (dashed). Note that the data in the red region were acquired with a sample of concentration *ca.* ten times that used for the blue region so that quantitative comparison of the absorption changes in the two regions should not be made. The insets show representative kinetic traces at 510–515 nm. Only the first 200 ps are shown, because from 200 ps to 3 ns there is no further change due to the long lifetime (12–13 ns) of the excited Fb-porphyrin under these conditions. The curves through the kinetic data are fits to a single exponential function with time constants of 31 ± 3 ps (A) and 26 ± 3 ps (B) that represent the lifetime of the excited metalloporphyrin component of the dimer.

to $Q_x(0,1)$ stimulated emission from the Fb-porphyrin. The stimulated (by the white-light probe pulse) emission features are characteristic of the excited singlet states of the porphyrins and occur near the wavelengths of the features observed in the spontaneous emission (fluorescence) spectrum, as is observed for the dimers under investigation here.

Fig. 5A shows that at 100 ps the $Q_y(1,0)$ bleaching near 515 nm due to the Fb-porphyrin in MgFbU has grown in magnitude while bleaching of the Q(0,0) band near 560 nm of the Mg-porphyrin has decreased. Changes are also observed in the other regions of the spectrum. The differences between the spectra at 1 and 100 ps clearly reflect disappearance of the Mg-porphyrin excited state (Mg*) and the formation of the Fb-porphyrin excited state (Fb*) in that fraction of the dimers in which the Mg-porphyrin had been excited by the pump flash. Note, however, that the fraction in which the Fb* excited state was initially produced does not change over the *ca.* 3 ns timescale of the measurements because the Fb* lifetime in toluene is 12–13 ns, as determined by fluorescence methods (*vide infra*).

A representative kinetic trace is shown in the inset to Fig. 5A along with a fit to a single exponential function with a time constant of 31 ps. The same value (31 ± 4 ps) is found from analysis of the data at all wavelengths where sufficiently large absorption changes are observed. We assign this time constant as the Mg* lifetime for MgFbU in toluene.

The ZnFbU dimer in toluene shows similar results as observed for MgFbU. The transient absorption spectra and kinetic data in Fig. 5B are in excellent agreement with the data presented for ZnFbU previously.[13] The observed lifetime of the Zn-porphyrin excited state of 26 ± 3 ps is the same within experimental error as the value of 22 ± 2 ps obtained previously. In analogy with the above results on MgFbU, this time constant reflects the energy-transfer process Zn*Fb→ZnFb*. The lifetimes of the pentameric arrays and representative monomers were also collected in toluene (Table 4). Each pentamer (Mg_4FbU, Zn_4FbU) shows a metalloporphyrin lifetime that is slightly shorter than that observed in the respective dimer.

The excited-state lifetimes of the metalloporphyrin (M*) in the MgFbU and ZnFbU dimers were examined in polar solvents (Table 4). In acetone and DMSO, MgFbU and ZnFbU each exhibit essentially the same lifetime as observed in toluene. In 2-nitrotoluene, MgFbU and ZnFbU each exhibited lifetimes of *ca.* 8 ps; however, in this solvent, MgU and ZnU also exhibited dramatically shortened lifetimes (14 and 52 ps, respectively). The shortened lifetime of each metalloporphyrin (MgU, ZnU) indicates that the results observed in the dimers are attributable to solvent–porphyrin interactions rather than to enhanced energy-transfer rates or competitive electron-transfer pathways inherent in the dimers.

Time-resolved fluorescence. The lifetimes of the Fb-porphyrins in the arrays, and the metalloporphyrins in the MgU and ZnU monomers, were measured by time-resolved fluorescence spectroscopy. The results are summarized in Table 4. Also included in Table 4 are lifetimes obtained previously in toluene and DMSO for the ZnFbU dimer and the ZnU and FbU control complexes.[13] These values and those obtained here for these systems are in excellent agreement. For example, the fluorescence lifetime of 13.1 ± 0.6 ns obtained here for the Fb-porphyrin emission in the ZnFbU dimer in toluene is the same within experimental error as the value of 12.5 ± 0.2 ns obtained previously from time-correlated single photon counting measurements. The same lifetime is found for FbU in toluene (13.3 *vs.* 12.5 ns). The lifetime of the Fb-porphyrin in MgFbU in toluene is the same again (13.1 ns). The finding of the same lifetime (12–13 ns) of the excited singlet state of the Fb-porphyrin in the monomer and dimers is in full accord with the observation that the fluorescence yield ($W_f \# 0.12$) is basically the same in these molecules (Table 3 and ref. 13). Collectively, these results demonstrate that neither the Zn- nor Mg-porphyrin in these dimeric arrays in non-polar media introduces any new decay channels that compete effectively with the inherent decay routes (fluorescence, internal conversion, intersystem crossing) of the Fb-porphyrin. The lifetime observed for the Fb-porphyrin in each of the pentamers (Mg_4FbU and Zn_4FbU) is shorter than that of the FbU-core porphyrin and of the Fb-porphyrin in the dimers (Table 3). The shortened values could be due to a quenching process or an altered structure of the core Fb-porphyrin due to the presence of the four appended metalloporphyrins.

As the polarity of the solvent increases, the lifetime of the Fb-porphyrin in the dimers becomes shorter. For example, the

Table 4 Excited-state lifetimes of metallo- (M) and free-base (Fb) porphyrins (296 K)[a]

	toluene		EA[b]	THF		acetone		2-nitrotoluene		acetonitrile		DMSO	
compound	M	Fb	Fb	M	Fb	M	Fb	M	Fb	M	Fb	M	Fb
MgFbU	31 ps	13.1 ns	13.8 ns	34 ps	12.8 ns	37 ps[c]	6.5 ns	9 ps	2.2 ns 2.0 ns[d]		3.8 ns	31 ps	1.3 ns 1.8 ns[d]
ZnFbU	26 ps 22 ps[e]	13.1 ns 12.5 ns[e]	13.5 ns		13.3 ns	30 ps[c]	11.7 ns	8 ps	4.4 ns 4.5 ns[d]		7.3 ns	 23 ps[e]	4.3 ns 4.8 ns[e]
Mg_4FbU	23 ps	10.7 ns											
Zn_4FbU	17 ps	10.6 ns											
MgU	10.0 ns			9.7 ns		9.8 ns		14 ps		9.6 ns		8.4 ns	
ZnU	2.5 ns 2.4 ns[e]			2.6 ns		2.7 ns		52 ps		2.4 ns		2.4 ns 2.3 ns[e]	
FbU		13.3 ns	13.8 ns		13.7 ns		13.6 ns		12.3 ns		13.5 ns		13.0 ns 12.6 ns[e]
FbU-core		12.5 ns											
MgTPP	8.3 ns												
ZnTPP	2.2 ns							2.1 ns		2.1 ns			

[a]The lifetimes of the excited metalloporphyrin in the dimers and pentamers were determined using transient absorption spectroscopy. The lifetimes for the excited Fb-porphyrin monomers, metalloporphyrin monomers, and the Fb-porphyrins in the dimers were obtained by time-resolved fluorescence spectroscopy. The error limits for the lifetimes obtained by time-resolved fluorescence spectroscopy are $\pm 5\%$ and those from time-resolved absorption spectroscopy are $\pm 10\%$. [b]Data reported only for the Fb-porphyrin in ethyl acetate. [c]A slightly longer value (*ca.* 60 ps) is measured in the range 450–500 nm, whereas the reported value was obtained at 515 nm. In all other solvents, the same lifetime was observed at all wavelengths between 450 and 550 nm. Because the same *ca.* 30 ps value is measured in the 515 nm region in all the solvents, we believe that this value reflects the excited metalloporphyrin lifetime in all of the media, and the slower kinetics measured in acetone in the blue region involve some other processes that do not affect the excited metalloporphyrin lifetime. [d]These values, also obtained from transient absorption spectroscopy, are only rough estimates because the kinetic data did not span a sufficient time span for an accurate determination. [e]These values are reproduced from a previous study[13] and are in good agreement with the values obtained here.

lifetime of the Fb-porphyrin in MgFbU in acetonitrile is 3.8 ns, which is a factor of 3.4 shorter than the value in toluene. This result parallels the behaviour observed for the fluorescence yields (Table 3, Fig. 3). Qualitatively similar results are obtained with ZnFbU, though the extent of quenching is less than with MgFbU. We attribute the yield and lifetime reductions in polar media to charge-transfer quenching of the Fb-porphyrin excited state.

Discussion

Zinc has been widely employed as a surrogate for magnesium in the preparation of porphyrin-based synthetic models of chlorophylls.[26] Our new synthetic methods for preparing Mg-porphyrins and Mg-containing porphyrin arrays obviate the reliance on Zn-porphyrins and shift the focus in light-harvesting or molecular photonics applications from the question of 'What is synthetically feasible?' to the design issue of 'Which metal exhibits more desirable photochemical and materials properties?' We have explored the latter issue by examining the pairwise interactions between metalloporphyrins (Mg, Zn) and Fb-porphyrins in dimers and star-shaped pentamers. These studies serve as a prelude to the design and preparation of larger multiporphyrin arrays. The major photochemical results from this comparative study are as follows. (1) The choice of metal ion (Mg^{II} *vs.* Zn^{II}) does not appreciably affect the rate of energy transfer in the arrays. The similarity in rates of energy transfer for the Mg- and Zn-containing arrays is attributed to the fact that the electronic coupling between the metalloporphyrin and Fb-porphyrin is approximately the same for Mg- *vs.* Zn-containing arrays. (2) The quantum yields of energy transfer are $\geqslant 99\%$ for arrays containing either metal ion. However, the yield of energy transfer is slightly higher in the Mg- *vs.* Zn-containing arrays owing to the longer intrinsic lifetime of the former metalloporphyrin. (3) Solvent polarity and changes in coordination geometry of the Mg- or Zn-porphyrin have very little effect on the rates and yields of energy transfer. (4) Polar solvents diminish the fluorescence yield and lifetime of the excited Fb-porphyrin in arrays containing either Mg- or Zn-porphyrins. The magnitude of the diminution is greater for the Mg-containing arrays. These effects are attributed to charge-transfer quenching of the excited Fb-porphyrin by the adjacent metalloporphyrin. The enhanced quenching in the Mg-containing arrays is a result of the greater driving force for charge separation. In the following section, we discuss each of these points in more detail. Next, we compare the energy-transfer characteristics of our MgFb- or ZnFb-containing arrays with qualitatively similar phenomena exhibited by selected arrays made by other workers. Finally, we comment on the merits of Mg- *vs.* Zn-porphyrins for materials applications in the context of their photochemical properties and their differing stabilities.

Photochemical characteristics of Mg- *vs.* Zn-containing arrays

Energy transfer rates and yields. The static fluorescence yield and fluorescence excitation spectral measurements indicate that the yield of energy transfer is essentially quantitative in both the Mg- and Zn-containing arrays. In this regime of high efficiency, a precise determination of the yield is best obtained *via* time-resolved measurements. From the measured lifetime of the metalloporphyrin in an array ($t_{M}*$) and the lifetime of a benchmark monomeric porphyrin ($t^{0}_{M}*$), the rate constant for energy transfer (k_{EnT}) from M* to Fb and the yield of energy transfer (W_{EnT}) can be calculated as shown in eqn. (1) and (2).

$$k_{EnT} = (t_{M}*)^{-1} - (t^{0}_{M}*)^{-1} \quad (1)$$

$$W_{EnT} = k_{EnT} t_{M}* = 1 - t_{M}*/t^{0}_{M}* \quad (2)$$

These equations assume there are no other pathways for depopulating the excited metalloporphyin in the arrays other than the intrinsic processes (intersystem crossing, internal conversion, radiative decay) also present in the benchmark monomer. The close matching of the excitation spectra and absorption spectra for the arrays in diverse solvents indicates a high yield of energy transfer and supports this assumption. However, within experimental uncertainty we cannot exclude the possibility of a small amount ($\leqslant 10\%$) of electron transfer from the M* excited state.

The lifetimes observed for the metalloporphyrins in the arrays (Table 4) were used to compute the rates and yields of energy transfer in toluene (Table 5). For MgFbU, the lifetime of the Mg* ($t_{Mg}* = 31$ ps) gives k_{EnT} *ca.* $(31\ ps)^{-1}$ due to the inherent lifetime ($t^{0}_{Mg}*$) of 10.0 ns observed for Mg* in the MgU control compound. Similarly for ZnFbU, the lifetime of the Zn* ($t_{Zn}* = 26$ ps) gives k_{EnT} *ca.* $(26\ ps)^{-1}$ due to the inherent lifetime ($t^{0}_{Zn}*$) of 2.5 ns observed for Zn* in the ZnU control compound. Thus, the rate of energy migration is nearly identical in MgFbU and ZnFbU.

Although the rates of energy transfer are nearly identical for the Mg- and Zn-containing arrays, the yields differ slightly as these reflect the inherent lifetime of the metalloporphyrin excited state [eqn. (2)]. For MgFbU, W_{EnT} is *ca.* 99.7% (31 ps lifetime in MgFbU *vs.* 10 ns lifetime in MgU) while for ZnFbU, W_{EnT} is *ca.* 99.0% (26 ps lifetime in ZnFbU *vs.* 2.5 ns lifetime in ZnU). Thus the yield of energy transfer is greater for the Mg-containing array in spite of the marginally slower rate. Similar results are observed for the pentamers Zn_4FbU and Mg_4FbU, where a marginally faster rate [$(17\ ps)^{-1}$ *vs.* $(23\ ps)^{-1}$, respectively] is observed for the former but the latter gives the higher yield (99.3 *vs.* 99.8%, respectively). Thus, the general features observed for Mg- and Zn-containing arrays are quite similar.

The similarity in rates of energy transfer observed for the Mg- and Zn-containing arrays can be attributed to the fact that the electronic coupling between the metalloporphyrin and Fb-porphyrin is approximately the same for the Mg- *vs.* Zn-containing arrays. In this connection, our prior studies of a variety of ZnFb-dimers have shown that the predominant pathway for energy transfer involves a through-bond rather than a through-space mechanism.[13] The through-space energy-transfer rate was calculated to be $(720\ ps)^{-1}$ for the ZnFb-dimeric arrangement (which is substantially slower than the observed rates), and the MgFb-dimeric structure is expected to have the same through-space rate. The through-bond energy-transfer process is explicitly mediated by the nature of the conformational energy surface of the diarylethyne linker, which dictates the extent of electronic communication between the p systems of linker and porphyrin ring(s). The Raman intensity of the $n_{C\equiv C}$ mode of the arylethyne linker (relative to the n_2 mode of the porphyrin) was shown to be a convenient static spectroscopic signature of the extent of this electronic interaction.[14] In particular, the intensity of the $n_{C\equiv C}$ mode was shown to parallel the rate of energy transfer in a series of ZnFb dimers containing differing degrees of torsional constraint.[13,14] In the case of MgFbU *vs.* ZnFbU, the similarity in the relative intensities of the $n_{C\equiv C}$ modes again parallels the similarity in the rates of energy transfer. Collectively, these

Table 5 Calculated energy transfer rate constants and yields in toluene (298 K)[a]

	k_{EnT}	W_{EnT} (%)
MgFbU	$(31\ ps)^{-1}$	99.7
ZnFbU	$(26\ ps)^{-1}$	99.0
Mg_4FbU	$(23\ ps)^{-1}$	99.8
Zn_4FbU	$(17\ ps)^{-1}$	99.3

[a]Calculated from the excited-state lifetimes in Table 4 using eqn. (1)–(4).

Table 6 Calculated charge-transfer ($MFb^*\rightarrow MV^+FbV^-$) rate constants and yields (298 K)[a]

compound	process	toluene	ethyl acetate	THF	acetone	2-nitrotoluene	acetonitrile	DMSO
MgFbU	k_{Fb^*CT}	NA[b]	NA	$(195\ ns)^{-1}$	$(12.5\ ns)^{-1}$	$(2.7\ ns)^{-1}$	$(5.3\ ns)^{-1}$	$(1.4\ ns)^{-1}$
	W_{Fb^*CT} (%)	NA	NA	7	52	82	72	90
ZnFbU	k_{Fb^*CT}	NA	NA	$(456\ ns)^{-1}$	$(84\ ns)^{-1}$	$(6.9\ ns)^{-1}$	$(15.3\ ns)^{-1}$	$(6.4\ ns)^{-1}$
	W_{Fb^*CT} (%)	NA	NA	3	14	64	46	67

[a]Calculated from the excited-state lifetimes in Table 4 using eqn. (1)–(4). [b]Not applicable. The lifetime is the same as in the FbU control compound, indicating no charge transfer occurs in this solvent.

trends lead to the assessment that the extent of electronic coupling is similar in the Mg- and Zn-containing arrays.

Effects of solvent on photodynamics of energy transfer. The solubility of the arrays provides the opportunity for examining the effects of different media on the excited state photodynamics. Our previous study of ZnFbU showed that the energy-transfer rate changed by a factor of $\leqslant$2.5-fold upon changes in viscosity (fluid medium to rigid glass), temperature (298–150 K), or polarity (solvent static relative permittivity e = 2.38–46.7).[13] In MgFbU, the fluorescence yield and lifetime of the Mg-porphyrin are basically unchanged in going from toluene to acetone to DMSO, indicating that the rate of energy transfer is unaffected by this dramatic change in solvent polarity. Similar results were observed for ZnFbU.

Although the rates of energy transfer do not change with increased solvent polarity, the reasonably polar solvent 2-nitrotoluene is exceptional compared with the rest of the solvents in giving shortened lifetimes. In this solvent, the lifetimes of the MgU and ZnU control complexes are dramatically reduced (to 14 ps and 52 ps, respectively) from the lifetimes in toluene (10.0 and 2.5 ns, respectively). Thus, the similar shortening in the lifetimes in the arrays does not reflect enhanced energy transfer (or competitive electron transfer) but is a consequence of a direct quenching interaction with the 2-nitrotoluene which provides a very fast decay route for M*.

The invariance in rates of energy transfer upon changes in solvent is supported by the RR data. These data show that the magnitude of the electronic coupling in both the Mg- and Zn-containing arrays is not strongly affected by the nature of the solvent (polar *vs.* non-polar) or the coordination number of the metal ion (and hence the conformation of the porphyrin ring). The constancy of the electronic coupling under a variety of conditions has important implications for the interpretation of the effects of solvent on the photochemical properties of the arrays.

Effects of solvent on fluorescence of the Fb-porphyrin. Although the rate of energy transfer and the magnitude of electronic coupling remain constant upon changes in solvent, both the fluorescence yield and excited-state lifetime of the Fb-porphyrin are diminished in polar solvents. Together these observations lead to the assessment that the quenching phenomenon is best attributed to a charge-transfer process ($MFb^*\rightarrow MV^+FbV^-$) that occurs following energy transfer from the metallo(M)- to Fb-porphyrin (or following direct excitation of the Fb-porphyrin). The quenching of the Fb-porphyrin excited state must occur within its nominal 12–13 ns lifetime. A model that accounts for this quenching is shown in Scheme 5. We previously reported quenching of the Fb-porphyrin in ZnFbU in the polar solvent DMSO.[13] The more comprehensive data base reported here for ZnFbU along with

$$M^*Fb \xrightarrow{k_{EnT}} MFb^* \xrightarrow{k_{Fb^*CT}} M^{\cdot+}Fb^{\cdot-} \xrightarrow{k_{CR}} MFb$$

Scheme 5 Charge-transfer quenching of the excited Fb-porphyrin (Fb*) by the ground-state metalloporphyrin (M)

the data obtained for MgFbU allow a more in-depth analysis of the charge-transfer process.

The lifetime of the Fb-porphyrin emission in the dimeric arrays (t_{Fb^*}) and the fluorescence lifetime of the FbU control complex ($t^0_{Fb^*}$) can be used to determine the rate constant for charge-transfer quenching (k_{Fb^*CT}) and the yield for the quenching process (W_{Fb^*CT}) *via* eqn. (3) and (4) (Table 6).

$$k_{Fb^*CT} = (t_{Fb^*})^{-1} - (t^0_{Fb^*})^{-1} \quad (3)$$

$$W_{Fb^*CT} = k_{Fb^*CT} \cdot t_{Fb^*} = 1 - t_{Fb^*}/t^0_{Fb^*} \quad (4)$$

For example, MgFbU in acetonitrile has k_{Fb^*CT} *ca.* $(5.3\ ns)^{-1}$ and W_{Fb^*CT} *ca.* 72% under these conditions (the competing processes being fluorescence, internal conversion, and intersystem crossing), while ZnFbU in acetonitrile has k_{Fb^*CT} *ca.* $(15.3\ ns)^{-1}$ and W_{Fb^*CT} *ca.* 46%. The most polar solvent examined, DMSO, gives substantial quenching, with W_{Fb^*CT} *ca.* 90 and 67% for the MgFb- and ZnFb-dimers, respectively. Note that for both types of arrays, the values of k_{Fb^*CT} and W_{Fb^*CT} generally increase as the solvent polarity increases, though the trend is not exactly linear as 2-nitrotoluene quenches slightly more than expected given its polarity. There is no reason to expect this trend to follow the solvent polarity precisely, because other factors such as porphyrin electrochemical potentials are of critical importance in determining the extent of charge-transfer quenching, and these also are affected by the nature of the solvent.[23b]

Collectively, the analysis of the fluorescence yield (Fig. 3) and lifetime (Table 4) data of the MgFbU *vs.* ZnFbU array as a function of solvent polarity indicate that the charge-transfer process is more pronounced for the former arrays. The more facile charge-transfer quenching observed for MgFbU *vs.* ZnFbU is attributed to the larger driving force for the $MgFb^*\rightarrow MgV^+FbV^-$ process relative to the $ZnFb^*\rightarrow ZnV^+FbV^-$ reaction. This difference derives from the *ca.* 300 mV greater ease of oxidation of the Mg-porphyrin relative to the Zn-porphyrin.[10,23,32] Hence, Mg-containing arrays offer some advantage over Zn-containing arrays in situations wherein charge transfer is a desired property of the assembly.

Energy-transfer properties of other dimers

A large number of dimers have been prepared for studies of energy transfer, with most containing Zn- and Fb-porphyrins.[6,26] Among these, the most relevant to this discussion are those where charge-transfer quenching of the Fb-porphyrin has been observed. Also relevant are those arrays where energy transfer has been studied between Mg- and Fb-porphyrins, though these are far fewer in number.[28k,29a]

Gust *et al.* prepared a ZnFb-dimer joined by a phenyl–amide–phenyl linker and observed fast energy transfer [$k_{EnT} = (43\ ps)^{-1}$] with $W_{EnT} = 0.97$ in CH_2Cl_2.[45] A dimer with the same linker but electron-deficient substituents on the Fb-porphyrin exhibited slightly slower energy transfer [$k_{EnT} = (106\ ps)^{-1}$] which was competitive with electron transfer ($W_{ET} = 0.77$, $W_{ET} = 0.18$). In addition, the excited-state lifetime of the Fb-porphyrin was shortened from 8.5 to 2.7 ns which was attributed to charge-transfer quenching ($W_{Fb^*CT} = 0.68$).

Although both dimers were examined in the non-polar solvent CH_2Cl_2, the electron-deficient groups provide increased driving force for the charge-transfer process and thus play a role similar to that of a polar solvent in enhancing this process. Two related ZnFb-dimers, each with an electron-rich Zn-porphyrin and an electron-deficient Fb-porphyrin, were examined in a wide variety of solvents.[46] The charge-transfer quenching process of the Fb-porphyrin was not detected in toluene, became apparent in solvents such as ethyl acetate, and increased dramatically in rate upon going to polar solvents such as DMSO.

Several dimers[28] and trimers[29] containing Mg-porphyrins have been prepared, but in almost all cases electron transfer rather than energy transfer has been the dominant photochemical process. Osuka *et al.* prepared a series of MgFb dimers joined by hydrocarbon spacers of various lengths wherein energy transfer was studied.[28k] In one bis-spiroindane linked MgFb dimer examined in DMF, fast energy transfer [$k_{EnT} = (62\ ps)^{-1}$] and faster electron transfer [$k_{ET} = (42\ ps)^{-1}$] were observed with quantum yields of 0.4 and 0.6, respectively. In other MgFb dimers with assorted linkers, energy transfer occurred with no observable competing electron-transfer processes. In the series of MgFb dimers, the rates of energy transfer changed little (less than two-fold) in going from toluene to THF. In the same series in DMF, however, quenching of the Fb-porphyrin fluorescence was observed with a rate increasing with shorter linkers and this also was attributed to charge separation ($MgFb^* \rightarrow Mg^{+}Fb^{-}$) as proposed here.

Merits of Mg- *vs.* Zn-containing arrays for materials applications

Synthetic multiporphyrin nanostructures constitute a relatively new class of optical and photonic materials. The modularity of the building block approach enables relatively easy preparation of diverse composite arrays containing different metallo- or Fb-porphyrins. The studies reported herein indicate that the energy-transfer characteristics of the Mg-containing arrays are generally similar to those of their Zn-containing counterparts. The overall similarity in this property of the two types of arrays is on the surface surprising given the fact that magnesium (atomic number 12) is an alkaline earth metal while zinc (atomic number 30) is a transition metal with a filled 3d shell of electrons. For example, the Mg^{II} ion prefers an octahedral coordination sphere but also can accommodate a square-pyramidal geometry, while the presence of the malleable 3d shell of electrons in Zn^{II} leads to tolerance of a variety of coordination spheres. Nonetheless, Mg^{II} and Zn^{II} have nearly the same ionic radius (0.72 Å and 0.74 Å, respectively),[47] which is slightly larger than optimal for a comfortable fit in the porphyrin core.[48] Regardless, these basic differences in electronic structure and coordination-sphere geometry have very little influence on the linker-mediated electronic coupling between the metallo- and Fb-porphyrin which dictates the energy-transfer rates.

Certain differences do exist in the photochemical and materials properties of the Mg- *vs.* Zn-containing arrays. However, all of the differences can be directly traced to differences which are intrinsic to monomeric Mg- *vs.* Zn-porphyrins rather than being a consequence of array formation. These differences are as follows. (1) Although both Mg^{II} and Zn^{II} are diamagnetic and support metalloporphyrin singlet excited states with nanosecond lifetimes, Zn-porphyrins have a shorter lifetime (and commensurably diminished fluorescence yield) than Mg-porphyrins (2–2.5 ns *vs.* 8–10 ns, respectively). The shorter lifetime of Zn-porphyrins is due to the increased rate of intersystem crossing, which stems from the heavy-atom effect, not differences in radiative decay [MgTPP and ZnTPP have identical fluorescent radiative decay rates, k_f *ca.* $(60\ ns)^{-1}$].[36] (2) The somewhat increased charge-transfer propensity of the Mg-containing arrays is due to the fact that magnesium is less electronegative than zinc ($x = 1.31$ *vs.* 1.65); consequently, Mg-porphyrins are more easily oxidized than Zn-porphyrins. (3) Mg^{II} is a harder (less malleable) ion and strongly prefers oxygenic rather than nitrogenous ligands, while Zn^{II} is softer and has similar affinity for both.[49] This preference for ligand type and geometry leads to much easier acid-induced demetallation of Mg-porphyrins than Zn-porphyrins, a property with considerable practical implications (in chromatographic purification of the arrays, silica is sufficiently acidic to demetallate Mg- but not Zn-porphyrins; thus, the former generally cannot be chromatographed on silica).[33]

The view that emerges from the above considerations is that the construction of molecular photonic devices based on Mg- or Zn-porphyrins will be based on a host of factors in addition to the photochemical properties of the two types of arrays. Clearly, either metal ion could be used if the rate of energy transfer is the only factor to be considered. However, Mg-containing arrays may offer certain advantages in cases where a succession of energy-transfer steps occur. For example, assuming the yields observed for MgFbU (99.7%) and ZnFbU (99.0%) carry over to extended arrays of metalloporphyrins, then upon 100 transfer steps, the all-Mg-containing arrays would give 74% efficiency while the all-Zn-containing arrays would give 37% efficiency. Such a large number of transfer steps would be required in realistic models of the natural light-harvesting arrays. These considerations must be balanced with the fact that Mg-porphyrins are more prone to oxidation, and this must be suppressed in a light-harvesting array. Conversely, the propensity toward oxidation of Mg-porphyrins might be attractive in other types of devices such as switching elements. Indeed, we have applied the basic elements of this concept in the construction of a prototypical molecular optoelectronic gate.[10] Finally, from a processing or device packaging standpoint, Zn-porphyrins are more robust toward demetallation. However, Mg-chelates of electron-deficient porphyrins are less susceptible to demetallation than are those with electron-rich substituents. Thus, the incorporation of appropriate electron-withdrawing groups with the Mg-porphyrin may provide protection toward demetallation, charge transfer, and photooxidation while maintaining the desired long lifetime of the singlet excited state. All of these factors need to be considered in the design of metalloporphyrin-based light-harvesting arrays and nanostructures for materials applications.

Conclusions

Multiporphyrin arrays comprised of Fb- and Mg- or Zn-porphyrins can be constructed using a modular building block approach. No significant differences exist in the synthesis of Mg- or Zn-containing porphyrins or related arrays. Arrays containing Mg-porphyrins provide new models for biomimetic investigations of natural light-harvesting phenomena. In many regards, magnesium and zinc can be used almost interchangeably in many light-harvesting arrays. The choice of metal can be based on subtle factors such as the slightly faster rate of energy transfer provided by Zn-porphyrins, the slightly higher yield of Mg-porphyrins emanating from the inherently longer lifetime of Mg-porphyrins, or the desire to favour charge-transfer processes to which Mg-porphyrins are more inclined. Regardless, the choice of metal is now a design issue rather than a synthetic consideration. The ability to tune the photodynamic properties of the arrays through choice of metal is an important handle for controlling the flow of energy in porphyrin-based nanostructures. Finally, metalloporphyrins containing metals with far larger differences than magnesium and zinc should also be accessible *via* this modular synthetic approach, in turn broadening the scope of photonic and electronic properties that can be elicited in these porphyrin-based materials.

This work was supported by a grant from Division of Chemical Sciences, Office of Basic Energy Sciences, Office of Energy Research, Department of Energy (J.S.L.), the LACOR Program (D.F.B.) from Los Alamos National Laboratory, and grants GM36243 (D.F.B.) and GM34685 (D.H.) from the National Institute of General Medical Sciences. Laser desorption mass spectra were obtained by Dr. Walter Svec at Argonne National Laboratory.

References

1 (*a*) A. W. D. Larkum and J. Barrett, *Adv. Bot. Res*., 1983, **10**, 1; (*b*) *Photosynthetic Light-Harvesting Systems*, ed. H. Scheer and S. Siegried, W. de Gruyter, Berlin, 1988; (*c*) D. C. Mauzerall and N. L. Greenbaum, *Biochim. Biophys. Acta*, 1989, **974**, 119; (*d*) C. N. Hunter, R. van Grondelle and J. D. Olsen, *Trends Biochem. Sci*., 1989, **14**, 72; (*e*) G. McDermott, S. M. Prince, A. A. Freer, A. M. Hawethornthwaite-Lawless, M. Z. Papiz, R. J. Cogdell and N. W. Isaacs, *Nature* (*London*), 1995, **374**, 517; (*f*) S. Karrasch, P. A. Bullough and R. Ghosh, *EMBO J*., 1995, **14**, 631.

2 R. Jimenez, S. N. Dikshit, S. E. Bradforth and G. R. Fleming, *J. Phys. Chem*., 1996, **100**, 6825.

3 J. S. Lindsey, S. Prathapan, T. E. Johnson and R. W. Wagner, *Tetrahedron*, 1994, **50**, 8941.

4 S. Prathapan, T. E. Johnson and J. S. Lindsey, *J. Am. Chem. Soc*., 1993, **115**, 7519.

5 R. W. Wagner and J. S. Lindsey, *J. Am. Chem. Soc*., 1994, **116**, 9759.

6 R. W. Wagner, T. E. Johnson and J. S. Lindsey, *J. Am. Chem. Soc*., 1996, **118**, 11166.

7 N. Nishino, R. W. Wagner and J. S. Lindsey, *J. Org. Chem*., 1996, **61**, 7534.

8 J. S. Lindsey, in *Modular Chemistry*, ed. J. Michl, Kluwer Academic, Dordrecht, in press.

9 R. W. Wagner, T. E. Johnson, F. Li and J. S. Lindsey, *J. Org. Chem*., 1995, **60**, 5266.

10 R. W. Wagner, J. S. Lindsey, J. Seth, V. Palaniappan and D. F. Bocian *J. Am. Chem. Soc*., 1996, **118**, 3996.

11 D. Fenyo, B. T. Chait, T. E. Johnson and J. S. Lindsey, *J. Porph. Phthalocy*., 1997, **1**, 93.

12 J. Seth, V. Palaniappan, T. E. Johnson, S. Prathapan, J. S. Lindsey and D. F. Bocian, *J. Am. Chem. Soc*., 1994, **116**, 10 578.

13 J. S. Hsiao, B. P. Krueger, R. W. Wagner, T. E. Johnson, J. K. Delaney, D. C. Mauzerall, G. R. Fleming, J. S. Lindsey, D. F. Bocian and R. J. Donohoe, *J. Am. Chem. Soc*., 1996, **118**, 11 181.

14 J. Seth, V. Palaniappan, R. W. Wagner, T. E. Johnson, J. S. Lindsey and D. F. Bocian, *J. Am. Chem. Soc*., 1996, **118**, 11 194.

15 A. A. Bothner-By, J. Dadok, T. E. Johnson and J. S. Lindsey, *J. Phys. Chem*., 1996, **100**, 17 551.

16 (*a*) L. Milgrom, *J. Chem. Soc., Perkin Trans. 1*, 1983, 2535; (*b*) J. Davila, A. Harriman and L. R. Milgrom, *Chem. Phys. Lett*., 1987, **136**, 427.

17 (*a*) O. Wennerstrom, H. Ericssom, I. Raston, S. Svensson and W. Pimlott, *Tetrahedron Lett*., 1989, **30**, 1129; (*b*) A. Osuka, B. Liu and K. Maruyama, *Chem. Lett*., 1993, 949.

18 D. L. Officer, A. K. Burrell and D. C. W. Reid, *Chem. Commun*., 1996, 1657.

19 (*a*) T. Nagata, A. Osuka and K. Maruyama, *J. Am. Chem. Soc*., 1990, **112**, 3054; (*b*) K. Ichihara and Y. Naruta, *Chem. Lett*., 1995, 631.

20 (*a*) A. Osuka, N. Tanabe, R. P. Zhang and K. Maruyama, *Chem. Lett*., 1993, 1505; (*b*) A. Osuka, N. Tanabe, S. Nakajima and K. Maruyama, *J. Chem. Soc., Perkin Trans. 2*, 1996, 199; (*c*) S. Anderson, H. L. Anderson and J. K. M. Sanders, *Angew. Chem., Int. Ed. Engl*., 1992, **31**, 907.

21 H. Aota, Y. Itai, A. Matsumoto and M. Kamachi, *Chem. Lett*., 1994, 2043.

22 (*a*) S. Anderson, H. L. Anderson, A. Bashall, M. McPartlin and J. K. M. Sanders, *Angew. Chem., Int. Ed. Engl*., 1995, **34**, 1096; (*b*) H. L. Anderson, S. Anderson and J. K. M. Sanders, *J. Chem. Soc., Perkin Trans. 1*, 1995, 2231; (*c*) S. Anderson, H. L. Anderson and J. K. M. Sanders, *J. Chem. Soc., Perkin Trans. 1*, 1995, 2255; (*d*) E. Alessio, M. Macchi, S. Heath and L. G. Marzilli, *Chem. Commun*., 1996, 1411.

23 (*a*) D. G. Davis, in *The Porphyrins*, ed. D. Dolphin, Academic Press, New York, 1978, vol. 5, pp. 127–152; (*b*) R. H. Felton, in *The Porphyrins*, ed. D. Dolphin, Academic Press, New York, 1978, vol. 5, pp. 53–126.

24 W. R. Scheidt, in *The Porphyrins*, ed. D. Dolphin, Academic Press, New York, 1978, vol. 3, pp. 463–512.

25 M. Gouterman, in *The Porphyrins*, ed. D. Dolphin, Academic Press, New York, 1978, vol. 3, pp. 1–166.

26 For reviews, see: (*a*) S. G. Boxer, *Biochim. Biophys. Acta*, 1983, **726**, 265; (*b*) D. Gust and T. A. Moore, *Science*, 1989, **244**, 35; (*c*) V. V. Borovkov, R. P. Evstigneeva, L. N. Strekova and E. I. Filippovich, *Russ. Chem. Rev*., 1989, **58**, 602; (*d*) D. Gust and T. A. Moore, *Top. Curr. Chem*., 1991, **159**, 103; (*e*) M. R. Wasielewski, in *Chlorophylls*, ed. H. Scheer, CRC Press, Boca Raton, FL, USA, 1991, pp. 269–286; (*f*) M. R. Wasielewski, *Chem. Rev*., 1992, **92**, 435; (*g*) D. Gust, T. A. Moore and A. L. Moore, *Acc. Chem. Res*., 1993, **26**, 198; (*h*) S. E. Gribkova, R. P. Evstigneeva and V. N. Luzgina, *Russ. Chem. Rev*., 1993, **62**, 963; (*i*) H. Kurreck and M. Huber, *Angew. Chem., Int. Ed. Engl*., 1995, **34**, 849.

27 (*a*) K. N. Solovev, M. P. Tsvirko, A. T. Gradyushko and D. T. Kozhich, *Opt. Spectrosc*., 1972, **33**, 480; (*b*) T. Yamamura, *Chem. Lett*., 1977, 773; (*c*) K. Yamashita, N. Kihara, H. Shimidsu and H. Suzuki, *Photochem. Photobiol*., 1982, **35**, 1; (*d*) T. Katagi, T. Yamamura, T. Saito and Y. Sasaki, *Chem. Lett*., 1982, 417; (*e*) W. Szulbinski and M. Lapkowski, *Inorg. Chim. Acta*, 1986, **123**, 127; (*f*) K. Takahashi, H. Katsurada, T. Komura and H. Imanaga, *Bull. Chem. Soc. Jpn*., 1990, **63**, 3315; (*g*) S. Yamauchi, T. Ueda, M. Satoh, K. Akiyama, S. Tero-Kubota, Y. Ikegami and M. Iwaizumi, *J. Photochem. Photobiol. A: Chem*., 1992, **65**, 177; (*h*) Y. Iseki and S. Inoue, *J. Chem. Soc., Chem. Commun*., 1994, 2577; (*i*) K. Wynne, S. M. LeCours, C. Galli, M. J. Therien and R. M. Hochstrasser, *J. Am. Chem. Soc*., 1995, **117**, 3749.

28 (*a*) S. G. Boxer and G. L. Closs, *J. Am. Chem. Soc*., 1976, **98**, 5406; (*b*) C. K. Chang, *J. Heterocycl. Chem*., 1977, **14**, 1285; (*c*) M. R. Wasielewski, W. A. Svec and B. T. Cope, *J. Am. Chem. Soc*., 1978, **100**, 1961; (*d*) T. L. Netzel, P. Kroger, C. K. Chang, I. Fujita and J. Fajer, *Chem. Phys. Lett*., 1979, **67**, 223; (*e*) M. R. Wasielewski and W. A. Svec, *J. Org. Chem*., 1980, **45**, 1969; (*f*) T. L. Netzel, M. A. Bergkamp, C. K. Chang and J. Dalton, *J. Photochem*., 1981, **17**, 451; (*g*) I. Fujita, J. Fajer, C. K. Chang, C. B. Wang, M. A. Bergkamp and T. L. Netzel, *J. Phys. Chem*., 1982, **86**, 3754; (*h*) T. L. Netzel, M. A. Bergkamp and C. K. Chang, *J. Am. Chem. Soc*., 1982, **104**, 1952; (*i*) R. E. Overfield, A. Scherz, K. J. Kaufmann and M. R. Wasielewski, *J. Am. Chem. Soc*., 1983, **105**, 4256; (*j*) H. Kamogawa, S. Miyama and S. Minoura, *Macromolecules*, 1989, **22**, 2123; (*k*) A. Osuka, F. Kobayashi, K. Maruyama, N. Mataga, T. Asahi, T. Okada, I. Yamazaki and Y. Nishimura, *Chem. Phys. Lett*., 1993, **201**, 223; (*l*) P. Hilderbrandt, H. Tamiaki, A. R. Holzwarth and K. Schaffner, *J. Phys. Chem*., 1994, **98**, 2192; (*m*) H. Nakamura, M. Terazima, N. Hirota, S. Nakajima and A. Osuka, *Bull. Chem. Soc. Jpn*., 1995, **68**, 2193; (*n*) H. Berg, M. Rachamim, T. Galili and H. Levanon, *J. Phys. Chem*., 1996, **100**, 8791.

29 (*a*) S. G. Boxer and R. R. Bucks, *J. Am. Chem. Soc*., 1979, **101**, 1883; (*b*) R. R. Bucks, T. L. Netzel, I. Fujita and S. G. Boxer, *J. Phys. Chem*., 1982, **86**, 1947; (*c*) A. Osuka, B. Liu and K. Maruyama, *J. Org. Chem*., 1993, **58**, 3582; (*d*) A. Osuka, S. Marumo, S. Taniguchi, T. Okada and N. Mataga, *Chem. Phys. Lett*., 1994, **230**, 144; (*e*) Y. Kobuke and H. Miyaji, *Bull. Chem. Soc. Jpn*., 1996, **69**, 3563.

30 (*a*) H. Miyaji, Y. Kobuke and J. Kondo, *Chem. Lett*., 1996, 497; (*b*) H. Tamiaki, M. Amakawa, Y. Shimono, R. Tanikaga, A. R. Holzwarth and K. Schaffner, *Photochem. Photobiol*., 1996, **63**, 92.

31 (*a*) A. T. Gradyushko and M. P. Tsvirko, *Opt. Spectrosc*., 1971, **31**, 291; (*b*) A. Harriman, *J. Chem. Soc., Faraday Trans. 2*, 1981, **77**, 1281; (*c*) T. G. Politis and H. G. Drickamer, *J. Chem. Phys*., 1982, **76**, 285; (*d*) O. Ohno, Y. Kaizu and H. Kobayashi, *J. Chem. Phys*., 1985, **82**, 1779.

32 (*a*) J. H. Fuhrhop and D. Mauzerall, *J. Am. Chem. Soc*., 1969, **91**, 4174; (*b*) J. H. Fuhrhop, *Z. Naturforsch., Teil B*, 1970, **25**, 255; (*c*) N. Carnieri and A. Harriman, *Inorg. Chim. Acta*, 1982, **62**, 103.

33 J. S. Lindsey and J. N. Woodford, *Inorg. Chem*., 1995, **34**, 1063.

34 D. F. O'Shea, M. A. Miller, H. Matsueda and J. S. Lindsey, *Inorg. Chem*., 1996, **35**, 7325.

35 A. J. Gordon and R. A. Ford, in *The Chemist's Companion*, Wiley Interscience, New York, 1972, pp. 374–375.

36 P. G. Seybold and M. Gouterman, *J. Mol. Spectrosc*., 1969, **31**, 1.

37 M. D. Ediger, R. S. Moog, S. G. Boxer and M. D. Fayer, *Chem. Phys. Lett*., 1982, **88**, 123.

38 J. A. Riddick and W. B. Bunger, *Organic Solvents, Techniques of Chemistry*, Wiley-Interscience, New York, 3rd edn., 1970 vol. 2.

39 C. Kirmaier and D. Holten, *Biochemistry*, 1991, **30**, 609.

40 T. E. Johnson, Ph.D. Thesis, Carnegie Mellon University, 1995, p. 149.

41 H. Brochmann and N. Risch, in *Chlorophylls*, ed. H. Scheer, CRC Press, Boca Raton, FL, 1991, p. 108.

42 (*a*) R. P. Haugland, J. Yguerabide and L. Stryer, *Proc. Natl. Acad.*

Sci. USA, 1969, **63**, 23; (*b*) L. Stryer and R. P. Haugland, *Proc. Natl. Acad. Sci. USA*, 1967, **58**, 719.
43 J. S. Lindsey, P. A. Brown and D. A. Siesel, *Tetrahedron*, 1989, **45**, 4845.
44 J. Rodriguez, C. Kirmaier and D. Holten, *J. Am. Chem. Soc*., 1989, **111**, 6500.
45 D. Gust, T. A. Moore, A. L. Moore, F. Gao, D. Luttrull, J. M. DeGraziano, X. C. Ma, L. R. Makings, S. J. Lee, T. T. Trier, E. Bittersmann, G. R. Seely, S. Woodward, R. V. Bensasson, M. Rougée, F. C. De Schryver and M. Van der Auweraer, *J. Am. Chem. Soc*., 1991, **113**, 3638.
46 J. M. DeGraziano, A. N. Macpherson, P. A. Liddell, L. Noss, J. P. Sumida, G. R. Seely, J. E. Lewis, A. L. Moore, T. A. Moore and D. Gust, *New J. Chem*., 1996, **20**, 839.
47 N. N. Greenwood and A. Earnshaw, *Chemistry of the Elements* Pergamon, Oxford, 1984.
48 J. W. Buchler, in *The Porphyrins*, ed. D. Dolphin, Academic Press, New York, 1978, vol. 1, pp. 389–483.
49 J. Bjerrum, *Metal Ammine Formation in Aqueous Solution*, P. Haase and Sons, Copenhagen, 1957, pp. 137–164.

Paper 7/00146K; *Received* 7*th January*, 1997